Coordination Chemistry Reviews, 48 (1983) 203–242
Elsevier Scientific Publishing Company, Amsterdam – Printed in The Netherlands

TAKING METAL ATOM CHEMISTRY OUT OF THE COLD

GEOFFREY A. OZIN *, MARK P. ANDREWS, LINDA F. NAZAR, HELMUT X. HUBER and COLIN G. FRANCIS

Lash Miller Chemical Laboratories, University of Toronto, Toronto, Ontario M5S 1A1 (Canada)

(Received 18 June 1982)

CONTENTS

A. INTRODUCTION

Metal vapour chemistry from its very inception in the late sixties has carried through to the eighties the reputation of requiring high temperature sources for the generation of metal atomic reagents and cryogenic devices for the trapping and investigation of reactive intermediates and products [1]. In actual fact recent research has adequately demonstrated that neither very high nor very low temperature methods are necessary conditions for performing synthesis with metal atoms. The ability to manipulate the chemical reactions of metal atoms either with themselves to produce well defined metal clusters or with selected ligands to produce desirable chemicals, at ambient temperatures, is an important scientific goal in the quest for new materials of technological significance.

Traditionally, the association of metal atoms with either metal atoms or ligands, has been effected by cocondensing reagents either on a liquid nitrogen 77 K cooled surface of a static or rotary reactor designed for gram

0010-8545/83/$12.00 © 1983 Elsevier Science Publishers B.V.

scale preparative chemistry, or on a cryostatically cooled 4.2–10 K optical window for in situ microscale spectroscopy of different types.

In an effort to surmount the sampling problems associated with involatile or temperature sensitive ligands, solid state reactions, condensed phase inhomogeneities, uncertainties in melt down chemistry and general handling of products, Mackenzie and Timms [2] developed the metal vapour rotary solution reactor. Using cocondensation and solution phase methods, many different classes of metal atom reaction type were discovered, examples of which are listed below:

(a) Abstraction

$$2\ Cu + 2\ BCl_3 \xrightarrow{77\ K} 2\ CuCl + B_2Cl_4$$

(b) Electron transfer

$$Fe + Cp_2Mo_2(CO)_6 \xrightarrow[2Me\text{-}THF]{140\ K} [Fe(2Me\text{-}THF)_6][CpMo(CO)_3]_2$$

(c) Oxidative addition

$$Ni + C_6F_5Br \xrightarrow{77\ K} C_6F_5NiBr$$

(d) Simple orbital mixing

$$Pt + O_2 + N_2 \xrightarrow{10\ K} Pt(O_2)(N_2)$$

(e) Substitution

$$8\ Li + CCl_4 \xrightarrow{77\ K} CLi_4 + 4\ LiCl$$

(f) Disproportionation

$$2\ Ni + 2\ C_6F_5Br \xrightarrow{77\ K} 2\ C_6F_5NiBr \rightarrow (C_6F_5)_2Ni + NiBr_2$$

(g) Ligand transfer

$$2\ Ni + (CH_2{=}CHCH_2)_4Sn \xrightarrow{77\ K} 2\langle(-Ni-)\rangle + Sn_x$$

(h) Metal atom agglomeration

$$Cu \xrightarrow[Ar,\ 12\ K]{Cu} Cu_2 \xrightarrow{Cu} Cu_3 \xrightarrow{Cu} Cu_4 \rightarrow \ldots Cu_n$$

(i) Metal atom photoaggregation

$$Ag \xrightarrow[Xe,\ 12\ K]{h\nu(300\text{–}330nm)} Ag_2 \rightarrow Ag_3 \rightarrow Ag_4 \rightarrow \ldots Ag_n$$

(j) Metal cluster complexation

$$2\,V + 12\,CO \xrightarrow{12\,K} V_2(CO)_{12}$$

(k) Cluster complex formation

$$(\eta^6\text{-}C_6H_5CH_3)_2Mo + Mo \xrightarrow[MCH]{140\,K} (\eta\text{-}C_6H_5CH_3)_2Mo_2$$

(l) Metal cluster oxidative addition

$$Ni \rightarrow Ni_m \xrightarrow[77\,K]{C_nH_{2n+2}} Ni_mC_xH_y$$

(m) Excited state metal atom insertion

$$Cu(^2S)\{CH_4\} \xrightarrow[12\,K]{h\nu(320nm)} Cu(^2P)\{CH_4\} \rightarrow CH_3CuH$$

(n) Excited state metal atom insertion–dissociation

$$Cu(^2S)\{H_2\} \xrightarrow[Kr,\,12\,K]{h\nu(310nm)} Cu(^2P)\{H_2\} \rightarrow Cu(^2D)\{H_2\} \rightarrow CuH + H$$

Expectations of metal vapour synthesis (MVS) for providing straightforward avenues to a wide range of new transition metal based materials heightened rapidly in the early and mid-seventies, being encouraged by a number of interesting syntheses, some of which are shown in Fig. 1. Without exception, all of the materials shown in Fig. 1 were of basic interest to a multidisciplinary scientific audience and some were significant in a technological sense. All however, necessitated low temperature conditions for their synthesis and some required cryogenic methods for their stabilization, detection and characterization.

Although we were personally intrigued by the broadly based scientific ramifications of metal atom chemistry and endlessly fascinated by the associated spectroscopy, we experienced some frustration at being constantly forced to design and conduct experiments under cryogenic conditions. We sensed that the efforts to establish synthetic entries to a wide range of new materials were gradually being eroded by the impression of the complexity and esoteric nature of the experimental methods required to achieve the objectives. The combination of high and low temperature technologies seemed to present too high a barrier for MVS to gain general acceptance as a routine and useful method for the medium and large scale production of chemicals.

In an attempt to overcome some of the misgivings about the practical significance of MVS we initiated a programme of study in 1975 which specifically focussed attention on the effect of different matrix supports and reaction media for controlling the growth and stabilization of metal atomic, cluster and colloidal dispersions, with applications in catalysis in mind. Of

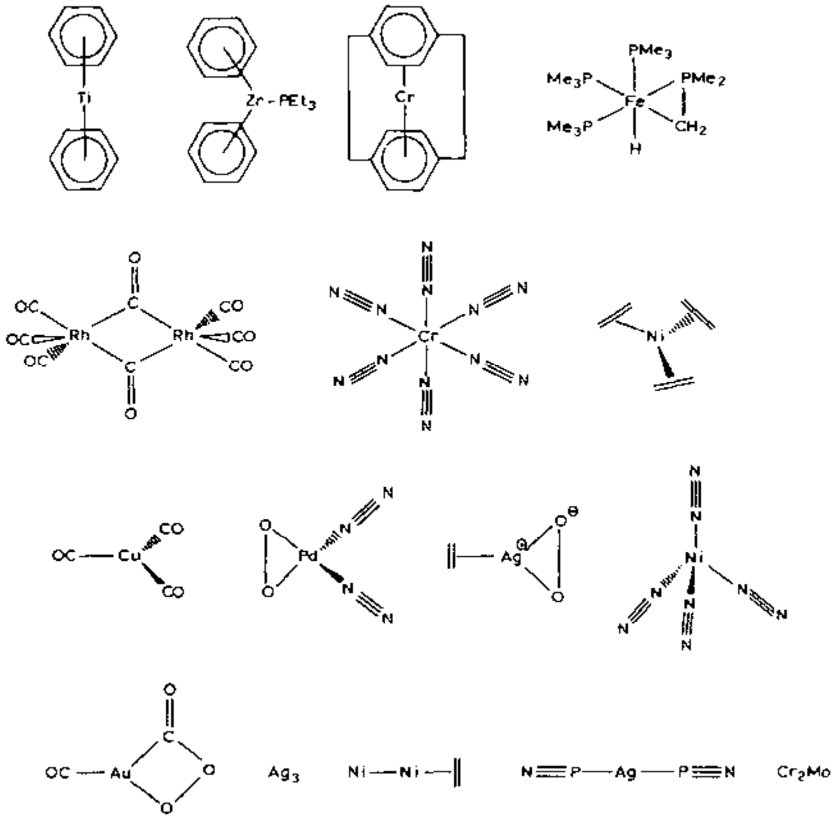

Fig. 1. Examples of molecules synthesized by macro- and matrix-scale metal vapor techniques (ref. 1).

the many possible candidates, alkanes, paraffin waxes, ice, polyethers and crown ethers, organic and inorganic polymers, inorganic oxides and zeolites, featured prominently on our list.

Some pivotal reports in the literature that influenced our thinking about ambient temperature MVS, included Kellerman and Texter's [3] study of small silver clusters grown by thermal autoreduction of silver ions in the supercages of zeolite Y; Grätzel and co-workers' proposed aza-crown ether stabilized silver atom produced by the photoreduction of the silver(I) precursor complex [4]; Symon and Forbes' [5] Ag_2^+, Ag_3^{2+} and Ag_4^{3+} silver cluster cations formed by γ-irradiation of silver(I) salts in frozen organic glassy solids; Vögtle and Weber's [6] long chain polyethers for selectively encapsulating not one, but two alkali metal ions; Klabunde et al.'s [7] discovery of solvated metal atoms and their use for preparing metal slurry catalysts; MacKenzie and Timms' [2] timely development of the rotary reactor technique for solution phase MVS; Blackborow et al.'s [8] observation of metal incorporation into polystyrene from Cr atom/styrene cocondensations; and the Francis and Timms' [9] report of involatile monomeric, oligomeric and polymeric ligands for MVS in the temperature range 140–250 K. Experiments of this kind provided many of the critical clues for developing the instrumentation and chemistry for taking MVS out of the cold.

The following is a brief and personal account of our ideas and efforts over the past five years, to establish a range of high temperature liquids and solutions suitable for performing ambient temperature MVS and to create supported metal compositions of a novel type. The utility of such reaction media for MVS will be determined by the following constraints: (i) the vapour pressure/viscosity/solubility characteristics of the medium over the working liquid range as these will define the temperature regime useful for synthetic preparations; (ii) the reactivity of the support towards the deposited metal atoms and/or clusters, as well as during any subsequent thermal and photolysis treatment; (iii) the nature of the metal atom and cluster support interactions, as these will influence the extent to which metal atom aggregation processes occur and the degree to which the spectroscopic and chemical properties of the atoms and clusters are perturbed by the medium; (iv) the thermal stability of metal atomic/cluster dispersions, indicated by the temperature above which desired or undesired diffusion/agglomeration processes became noticeable. Additional features which will figure in the viability of liquid and solution phase MVS approach include: (v) the availability of spectroscopic techniques for in situ monitoring of the fate of metal atoms deposited into solutions and liquids and therefore a means of quantifying the chemical events that occur in a macroscale rotary reactor synthesis; (vi) the practicality of a large scale preparation and the ability to conveniently manipulate the resulting products for chemical examination and catalytic screening.

Experience is proving that metal atom reactions with oligomeric and polymeric siloxanes, ethers and alkenes can lead to new classes of organometal polymers, polymer supported clusters and polymer protected colloids. The low vapour pressure/high viscosity characteristics of these liquids, the weakly solvating or complexing properties of the oxygen and olefinic backbones and the existence of pendant (or intrachain) functional groups, allows one to manipulate the diffusion, agglomeration and coordination behaviour of deposited metal atoms under ambient temperature conditions, in such a way that one can (in principle) design a specific metal-polymer composition for a particular application.

The fate of a metal atom deposited into a liquid polymer or a polymer in solution, will depend to a certain extent on the reactive pathways available to metal atoms, leading to self combination and interaction with monomers and oligomers, the latter representing solvating and ligating portions of the polymer. Metal atom-polymer chemistry performed to date has exploited interactions with ether and siloxane oxygens, olefinic, arene and cyclopentadiene functionalities. When metal atoms are deposited into an unfunctionalized poly(ethyleneglycol) or poly(dimethylsiloxane) liquid at 200–300 K, colloidal metal dispersions with broad particle size distributions are invariably formed in ways similar to those found for liquid and solid alkanes and waxes [11]. This is not too surprising as kinetic impediments have not been built into these polymeric supports to control the growth of and/or encourage the stabilization of metal monodispersions, subcolloidal agglomerates or small, well defined metal clusters. However, with the knowledge that arene ligands from relatively strongly bound complexes with the early transition metals and weakly bound complexes with the late ones, that cyclopentadiene forms a variety of fairly robust bonds to most transition metals, that olefinic groups bind firmly to many zerovalent transition metals (exceptions being, for example, Pd and Ag), and that ether/siloxane oxygen coordination to most low valent transition metals is expected to be of a highly labile type, it should be possible to prepare functionalized, solvating polymers which have the ability to direct metal atoms, clusters and colloids into chemically interesting environments. In what follows some of our studies of this type will be described.

B. RECENT SYNTHETIC, SPECTROSCOPIC AND KINETIC INVESTIGATIONS OF THE REACTIONS OF METAL ATOMS WITH POLY(DIMETHYL-CO-PHENYLMETHYL)SILOXANE

Francis and Timms [9] initially discovered that certain transition metal atoms could be reacted with liquid poly(dimethyl-co-phenylmethyl)siloxane DC510 ($\eta \sim 50$ centistokes, MW = ca. 3000, phenyl/methyl = ca. 1/17) at 250 K. The highly coloured and thermally stable (up to 200°C for M = Cr) product was formed in quantitative yield and was found to be an organometal liquid polymer, containing bis(arene) metal complexes, probably forming inter- and intramolecular cross links as illustrated in Scheme 1.

This finding can be considered to mark the beginning of a new phase in MVS. Here the experiments are performed at, or close to room temperature and involve the use of oligomeric and polymeric reagents containing different ligand types and mole fractions, having solvating or non-solvating backbones, exhibiting widely varying viscosities and possibly modified with various additives.

Following his thesis discovery, Dr. Colin Francis joined our research group at the University of Toronto in late 1978 eager to investigate a number of new avenues suggested by the M/DC510 system. Together with graduate

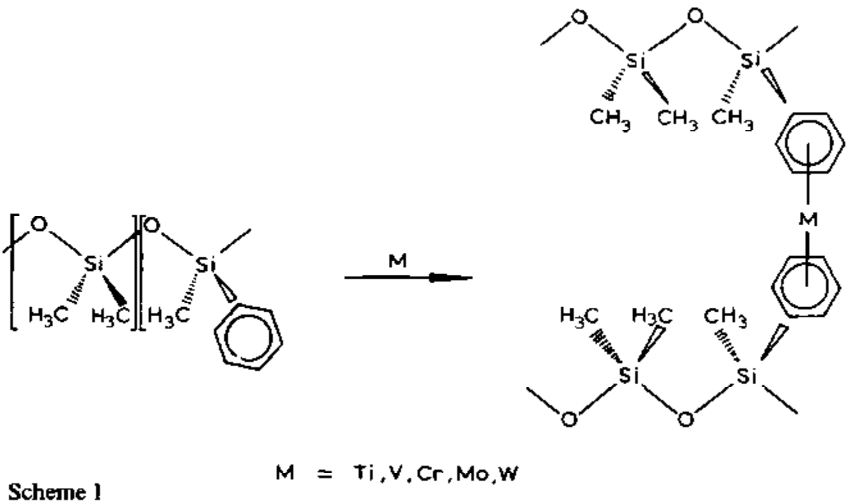

Scheme 1

students Mark Andrews and Linda Nazar and research associate Helmut Huber, we began a programme of investigation under the general theme "Metal Vapour Polymer Chemistry". Prior to the arrival of Francis we had developed a range of quantitative synthetic, spectroscopic and kinetic techniques for generating and identifying low nuclearity metal clusters of a unimetallic and multimetallic type in a range of low temperature matrix supports [12]. It therefore seemed clear, that a combination of macroscale metal liquid polymer methods with microscale spectroscopic probes, offered high potential for some interesting new discoveries. Out of these experiences grew metal vapour microliquid [13] and microsolution [14] optical and IR spectroscopy, which provided an invaluable in situ monitor of the fate of a metal atom reacting with liquid oligomeric or polymeric ligands, as well as ligands in various volatile solvents. The general methodology is illustrated in Fig. 2. Aside from allowing one to identify and quantify the chemical events leading to intermediates and products and to optimize product yields in a metal vapour rotary synthesis, this in situ metal atom reaction probe first brought to our attention the metal concentration dependence of the optical spectra of the M/DC510 system. A clear example can be seen in Mo/DC510 at 250 K illustrated in Fig. 3. The optical spectra of the metal vapour product represent four distinct growth stages indicated by absorbances at 418, 502, 578, 640 nm in addition to the MLCT absorption of the bis(arene) molybdenum centred at 318 nm [15]. Similar effects were observed with Ti, V and Cr in DC510 [16], as well as their bi-metal combinations [17]. An interesting early observation was that the order of appearance of these new species was opposite to the order of their thermal stabilities as seen from temperature dependent studies. Qualitatively, these results were taken to

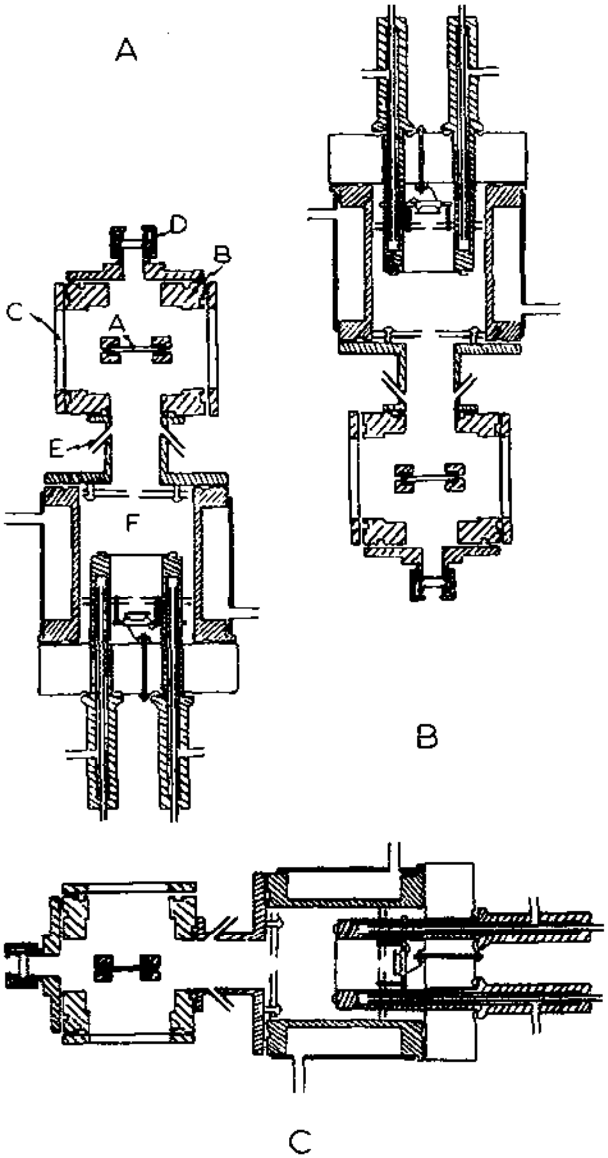

Fig. 2. Schematic representation of vacuum furnace-closed cycle helium refrigeration system used for metal vapor microliquid or microsolution optical spectroscopy as well as conventional metal vapor-matrix experiments: (A) NaCl or Suprasil optical window, horizontal configuration; (B) stainless-steel vacuum-shroud; (C) NaCl or Suprasil optical viewing ports; (D) Cajon-rubber septum, liquid or solution injection port; (E) gas deposition ports; (F) vacuum furnace and quartz crystal microbalance assembly. With the optical window in a fixed horizontal configuration, liquid or solution sample injection onto the window at any desired temperature in the range 12–300 K is performed in position A, metal deposition is conducted in position B and optical spectra are recorded in position C (ref. 14).

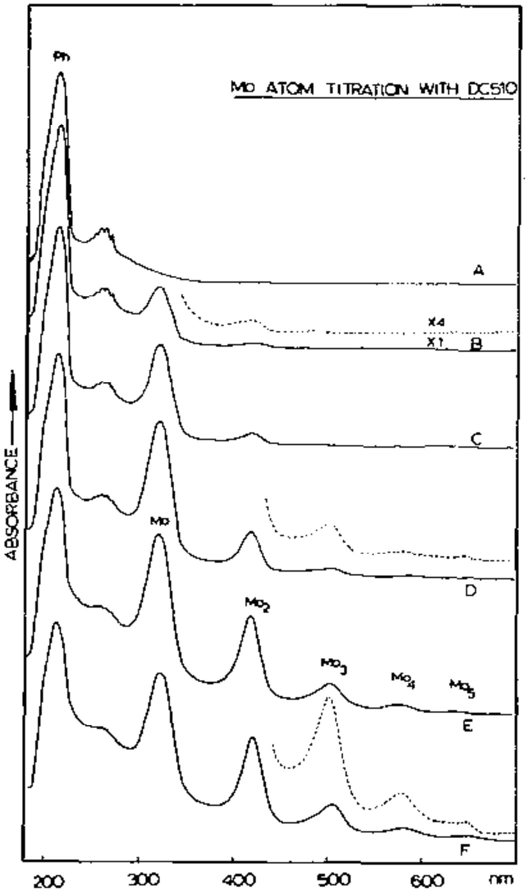

Fig. 3. Mo atom concentration study with DC510 at 250 K, UV-visible study. (A) neat liquid polymer film; (B)–(F) increasing concentration of Mo atoms (ref. 15).

indicate the formation and stabilization of small metal clusters, chemically or physically immobilized by the siloxane polymer [18]. Our goal from this point on was to develop spectroscopic, kinetic and chemical strategies which would enable us to directly probe the presumed metal atomic and cluster sites on the polymer; to establish cluster nuclearity; to elucidate the cluster growth and thermal agglomeration mechanisms; to define the role of phenyl substituents, bis(arene) metal crosslinking, solvating backbones; to examine the microdynamical properties of the polymers; to assess the homogeneity of the films and to achieve a chemical and/or physical separation of the various clusters for subsequent spectroscopic and crystallographic characterization. Our recent accomplishments in each of these areas will be briefly highlighted below.

A synthetic strategy for elucidating the nature of the metal cluster growth reactions in DC510 is laid out in Fig. 4, which represents a MVS temperature gradient varying from 293 to 10 K. Included in this study were a range of liquid arene functionalized ethers and siloxanes (A, B, D) of various chain lengths, alkanes (C, E), unreactive analogues containing only methyl functionalities, and arene/rare-gas (F) and rare-gas or alkane (G) solids. A

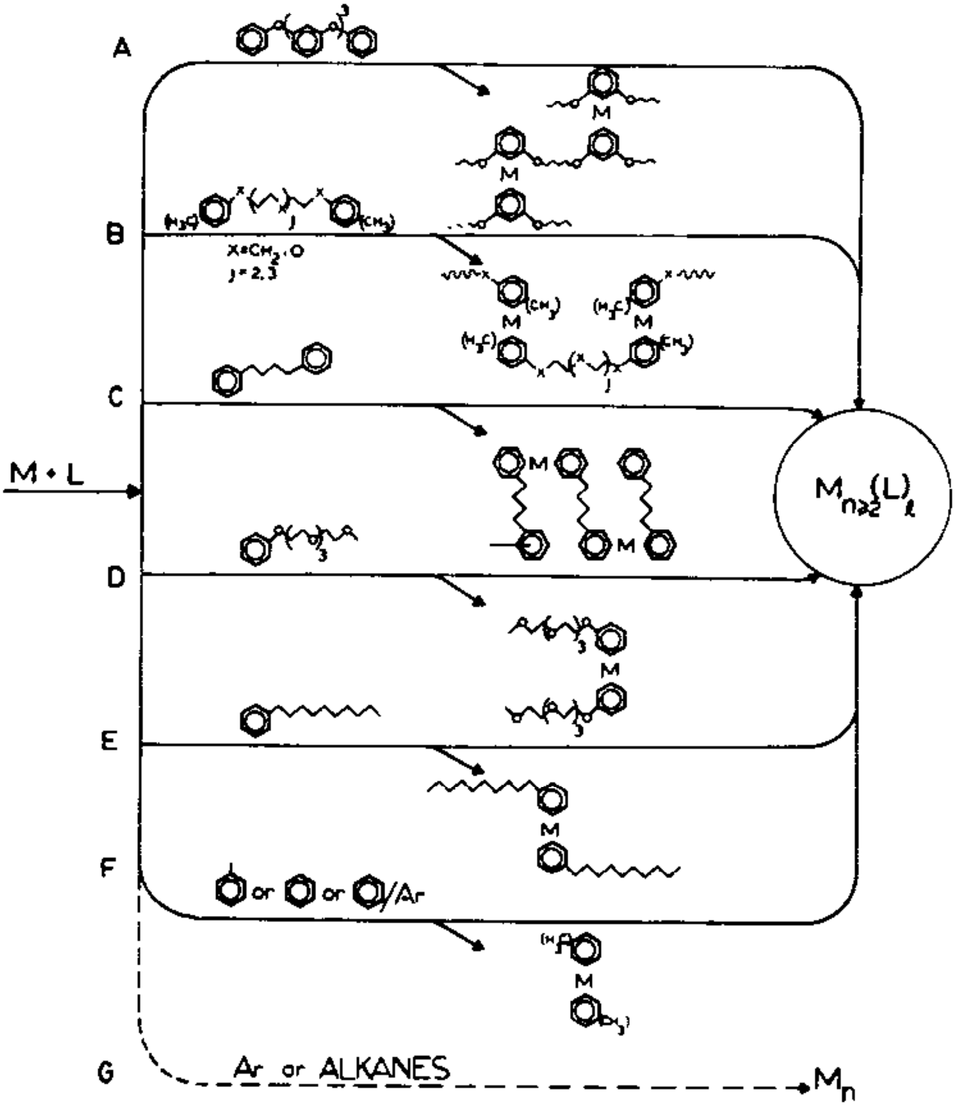

Fig. 4. Matrix- and macroscale metal vapor synthetic strategy used to elucidate the nature of metal cluster diffusion/agglomeration/complexation in DC510 (refs. 22,28,32,38).

typical series of room temperature titrations for Mo atoms into the seven oxygen α,ω-diphenylhexaethyleneoxide is shown in Fig. 5 and clearly displays the growth of the dimer and trimer stage. The importance of oxygen solvation was scrutinized with α,ω-ditolyldecane. The V_2, Cr_2 and Mo_2 clusters could be generated in this liquid medium. Clearly, the ability to establish an initial metal atom induced chain propagation step via bis-(arene) metal complex formation, was still possible in the α,ω-ditolyldecane ligand. The importance of this process in cluster formation and stabilization was assessed with an α-phenyldecane liquid sample (E). Dimetal cluster formation still occurs in this liquid. These observations first led us to believe that the dimetal clusters formed in DC510 were of a binary arene–metal

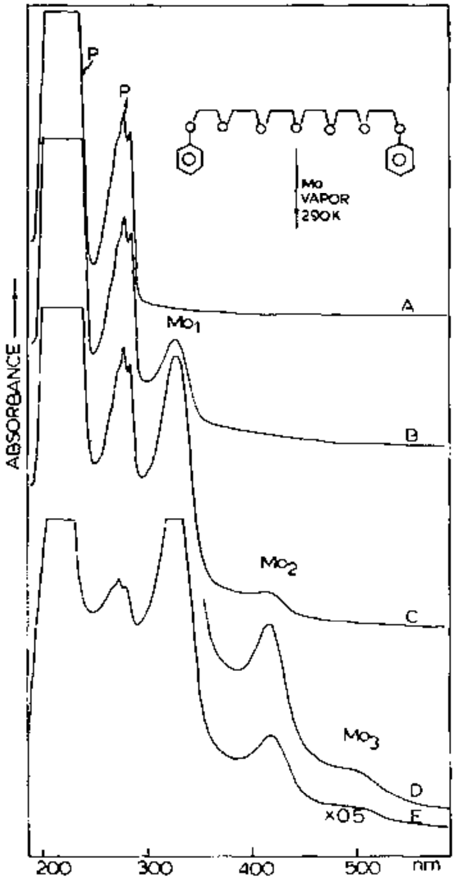

Fig. 5. UV-visible absorption spectroscopic study of the reaction of Mo atoms with α,ω-diphenylhexaethyleneoxide at 290 K: (A) pure oligomer; (B)–(D) increasing Mo atom concentration (ref. 32).

cluster type which would represent a new class of organometallic compound. Confirmation of this unexpected result stemmed from V atom cocondensation experiments in pure benzene and benzene/argon matrices at 12 K (F). A typical series of metal concentration experiments are depicted in Fig. 6A. These data are graphed in Fig. 6B as a function of the rate of metal atom deposition and are analysed using a kinetic model suitable for establishing metal cluster nuclearity [19]. The observed linear dependence of $\log[(\text{arene})_m V_n/(\text{arene})_2 V]$ versus $\log[V_0]$ with a slope of close to unity, unambiguously pinpoints the new arene-cluster species as $(\text{arene})_m V_2$. Similar results have also been obtained for Cr and Mo with benzene. Also the metal concentration dependence and spectroscopic similarity of the V/arene $\rightarrow (\text{arene})_2 V/(\text{arene})_m V_2$ matrix system to that of $V/CO \rightarrow V(CO)_6/V_2(CO)_{12}$ [20] is most noteworthy (Fig. 7). The presence of an optical transition around 460 nm for both $V_2(CO)_{12}$ and $(\text{arene})_m V_2$ suggests that this electronic excitation is probably metal localized in nature and characteristic of a V–V bonding interaction.

Recent experiments that have been designed to establish the arene coordination number *m* in $(\text{arene})_m M_2$ and provide further evidence for the M/DC510 reaction are laid out in Fig. 8A [22]. In these model metal atom-bis(arene) metal solution phase experiments, no evidence was found for free arene or metal displacement reactions or reduced products. Significantly, only a single product resulted from the $(\text{arene})_2 M + M'$ reaction (M, M′ = Cr or V) which was spectroscopically indistinguishable from the second product forming stage in the corresponding M/DC510 system. Hence we deduced that the first step in the agglomeration process involved the direct addition of a deposited diffusing metal atom to the metal centre of $(\text{arene}_2)M$ yielding the M_2, MM′ and M'_2 binuclear arene metal clusters, most likely having a symmetrical distribution of the arene rings with respect to the dimetal moiety as illustrated below. Such a structure for the dichromium complex is formally a 24-electron system, which can be considered to have at least a Cr≣Cr quadruple bond, with three π-electrons per arene ring contributing to each Cr atom. It is interesting that in tetrallyldichromium

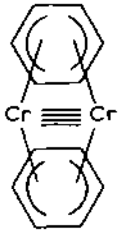

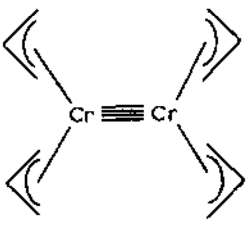

[23] four allyl ligands form a distorted tetrahedron around the two chromium atoms which are directly coupled over a distance of 1.97 Å. This short

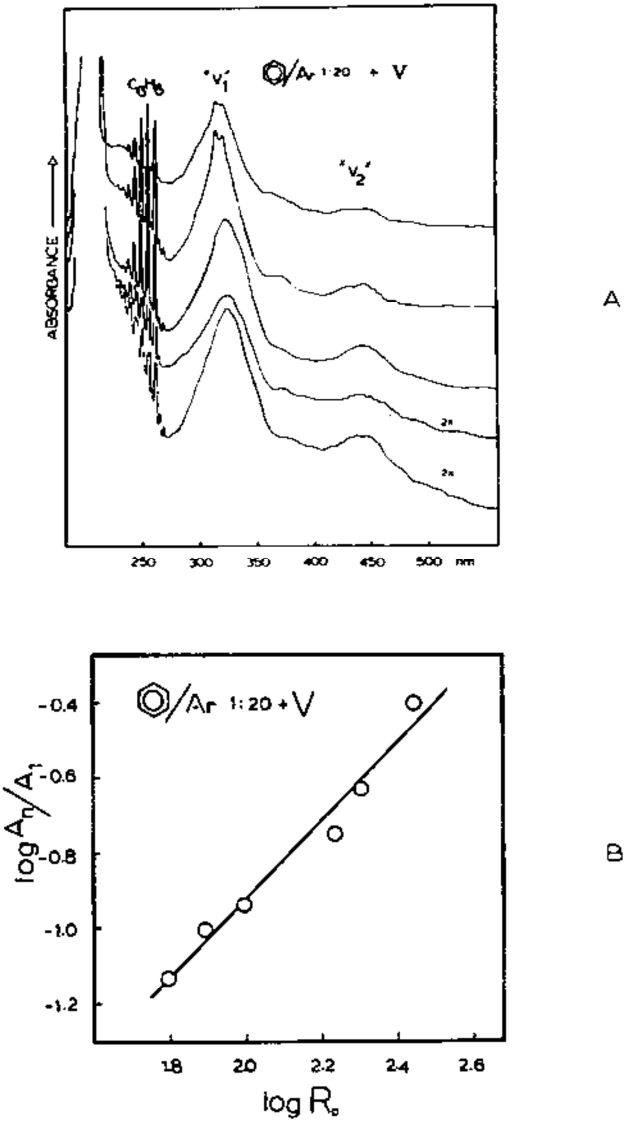

Fig. 6. (A) UV-visible spectroscopic vanadium atom concentration study with $C_6H_6/Ar = 1/20$ matrices at 12 K. Increasing metal concentration from top to bottom trace (ref. 38). (B) plot of the data in (A) based on the cluster agglomeration kinetic analysis of ref. 19, where $A_n = (C_6H_6)_mV_n$; $A_1 = (C_6H_6)_2V$; R_0 = rate of deposition of V atoms.

Cr–Cr bond should be compared to that of 1.85–2.54 Å found in other multiply bonded chromium dimers [24], to 1.86 Å for Cr_2 in solid Ar (EXAFS [25]) and to our preliminary EXAFS results for DC510 supported

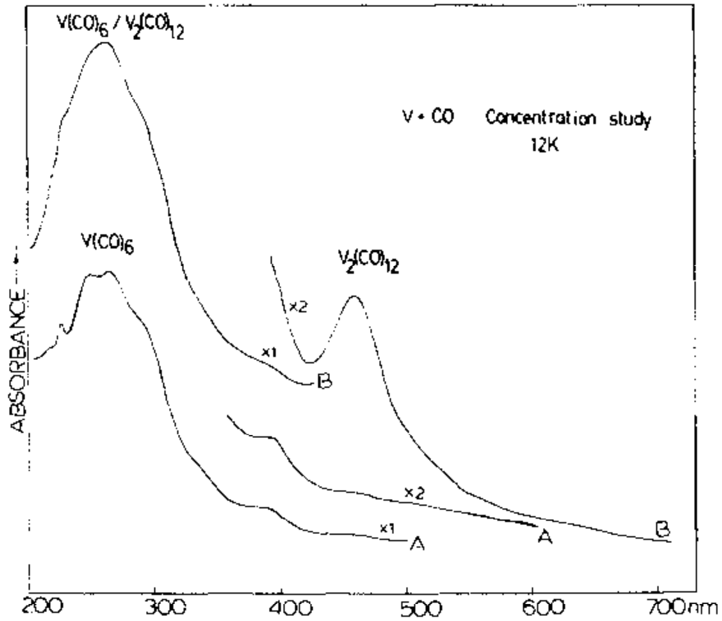

Fig. 7. UV-visible spectrum of the V/CO cocondensation reaction at 12 K: (A) V/CO ≅ $1/10^4$; (B) V/CO ≅ $1/10^3$ showing the conversion from $V(CO)_6$ to $V_2(CO)_{12}$. The band at about 460 nm is thought to be a metal localized electronic excitation associated with the V–V bond of the dimer (ref. 38).

Cr_2 which shows a Cr–Cr bond length in the range of 2 Å [26]. These observations support our earlier claims of low nuclearity cluster growth in DC510. Based on these new results, we propose that arene stabilized metal dimers and heterodimers are produced via a simple one-step addition of a metal atom to a bis(arene) metal target centre and that kinetically, the formation of dimers, trimers and higher clusters in DC510 is a birth and growth process, proceeding from a parent bis(arene) transition metal complex to higher nuclearity metal cluster compounds (involving a minimum of two arenes) through an array of parallel competitive addition reactions as illustrated in Fig. 8B [22]. Additional support for the formation of low nuclearity clusters in DC510 has also been obtained from recent SIMS [27] and laser Raman [28] studies of the Cr/DC510 and V/DC510 systems.

The Secondary Ion Mass Spectrometry (SIMS) experiment was initially calibrated by examining pure DC510 films at 12 K and freshly deposited Cr films at 12 K (Fig. 9A, C, D). The mass fragmentation patterns of these low temperature polysiloxane films were found to be surprisingly simple, showing very little structure above a mass number of 80. Sputtering of pure Cr

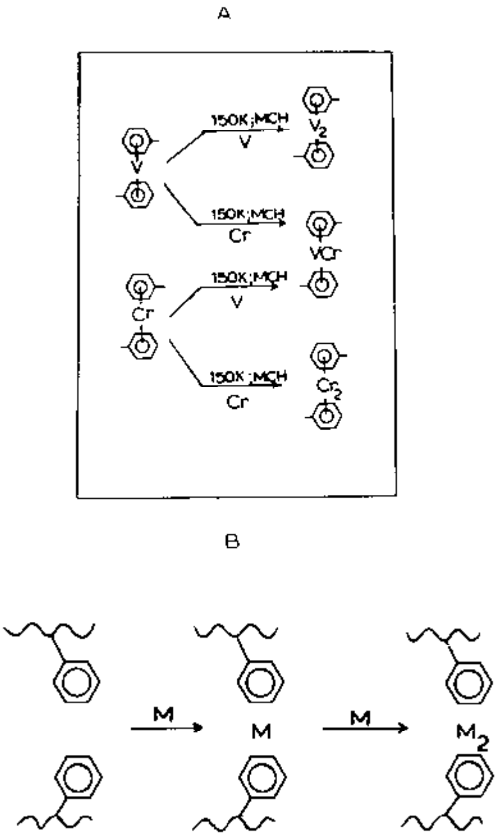

Fig. 8. (A) Synthetic strategy for the elucidation of the metal and ligand stoichiometry in binuclear arene-metal cluster complexes (refs. 22,32). (B) Metal nucleation model for the stepwise formation of arene-metal clusters in DC510 (refs. 22,32).

films showed evidence for Cr^+ and Cr_2^+ species in the ratio of roughly 100 : 1. Metal isotope structure was discernable in these spectra and assisted with the identification of sputtered ions (Fig. 9C, D). The SIMS recorded for the Cr/DC510 samples prepared at 250 K and recorded at 12 K, displayed remarkably constant depth profiles, pointing to impressive homogeneity of the films. Besides the mass peaks of the polymer, new lines were identified as Cr^+ and Cr_2^+ (Fig. 9B). The ion ratio of these metal species are roughly as found for the bulk metal; however, their ionization efficiency appears much higher. This is reasonable for the ejection and ionization of metal atoms and clusters having organometallic parentage rather than bulk or colloidal metal. These preliminary SIMS data for Cr/DC510 films can be considered to provide some support for our proposal of low nuclearity cluster growth and stabilization in the polymer.

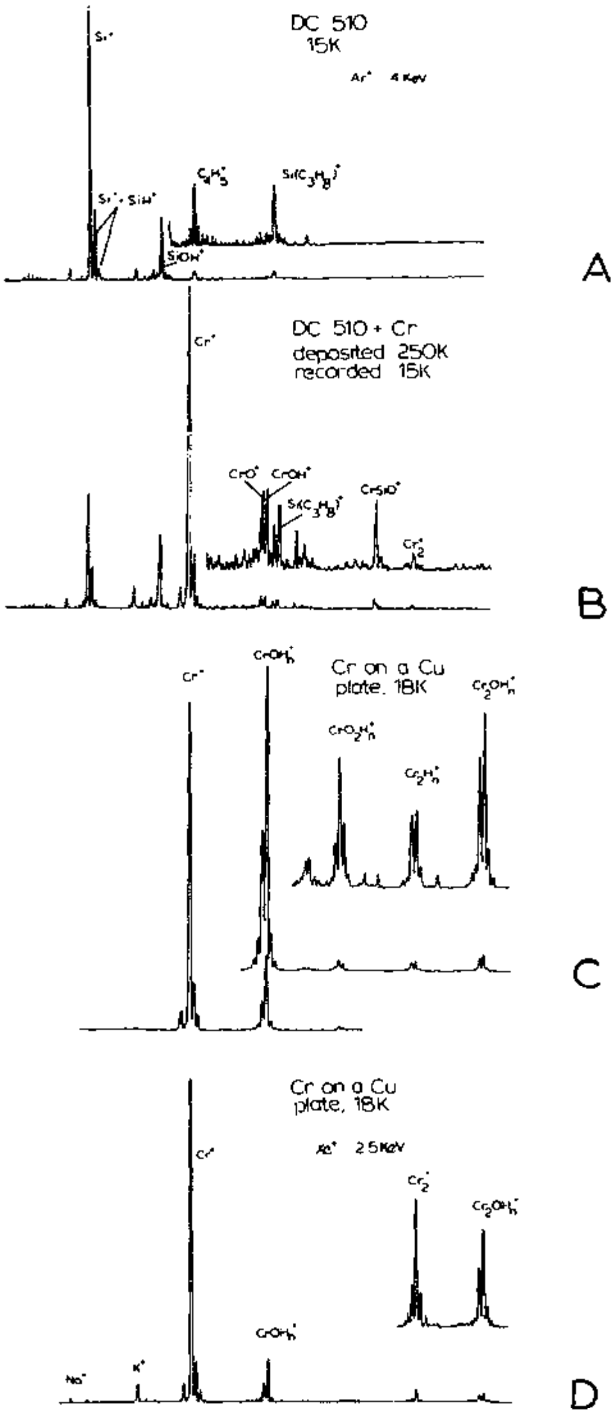

Fig. 9. Secondary ion mass spectra of: (A) DC510 film at 15 K; (B) Cr/DC510 film deposited at 250 K, recorded at 15 K; (C) Cr film deposited onto a Cu plate at 18 K, where (A) to (C) were recorded with 4KeV Ar^+; (D) Cr film deposited onto a Cu plate at 18 K recorded with a 2.5 KeV Xe^+ (ref. 27).

Vibrational spectroscopic studies are also proving useful for directly probing the metal–metal bonds of the polymer supported clusters. For example, the IR spectrum of the products of the V/DC510 reaction is congested with polymer absorptions [9,28] which obscure M-ring stretching and deformational modes expected in the 400–500 cm^{-1} region. In contrast, the low frequency Raman bands of the neat polymer [28] although rather broad, are few in number and occur at 490 (pol) and 180 (depol) cm^{-1}. For the polymer supported bis(arene) vanadium and divanadium compounds, new Raman bands appear at 520, 430, 270 and 155 cm^{-1}. All are polarized by comparison with the depolarized 180 cm^{-1} polymer reference line (Fig. 10). The bands at 520, 430 and 270 cm^{-1}, by analogy with the vibrational spectra of discrete bis(arene) metal sandwich complexes [29] are assigned to M–arene ring deformation and stretching motions. However, the band at 155 cm^{-1} has no counterpart in bis(arene) vanadium generated in a V/arene 77 K matrix or DC510 under mononuclear conditions, and therefore appears to be characteristic of the polymer supported divanadium species. In line with the low frequency Raman spectra of other M–M bonded cluster complexes [30], the intense, strongly polarized Raman line at 155 cm^{-1} is assigned to the symmetrical V–V stretching mode of DC510 supported divanadium.

ESR studies of the V/DC510 system are also proving to be most interesting [28,38]. In the case of a rigidly supported metal atomic or cluster reagent, the metal is held in a well defined environment. When the support is non-rigid, as is the case for DC510 above 150 K, the dynamic properties of the support will play an important role in the spectroscopy, metal atom chemistry and catalytic properties of the polymer. In the V/DC510 system, the V atom site on the polymer is paramagnetic and can function as an in situ spin probe of the polymer microdynamics over the entire time range of interest. A fairly concentrated sample of V/DC510 shows an anisotropic ESR spectrum below 300 K due to a matrix which varies from viscous to glassy as the temperature is lowered. The spectrum below 150 K displays 16 resolved vanadium hyperfine lines characteristic of a single unpaired electron coupling with an $I = 7/2$ V nucleus having axial symmetry (Fig. 11A). The form and temperature dependence of these spectra may be understood and the tumbling dynamics of the paramagnetic centre appreciated, by comparing it with the ESR spectrum of the corresponding unsupported bis(benzene) vanadium complex in a solid benzene matrix (12–77 K), Fig. 11A, and in pentane over the temperature range 120–300 K, Fig. 11B. From these data one can determine that the rotational correlation time of bis(arene) vanadium anchored to DC510 at around 300 K is comparable to that of bis(arene) vanadium in pentane around 130 K. Interestingly, the observation of anisotropic vanadium hyperfine lines yet essentially isotropic proton superhyperfine splitting for bis(benzene) vanadium in pentane at 123 K (Fig. 11B), implies free rotation of the complexed benzene rings with respect to a rigid molecular frame. However, the lack of resolvable proton superhyperfine splitting for bis(benzene) vanadium in solid benzene at 12–77 K, signals a totally rigid regime in which both molecular tumbling and coordinated

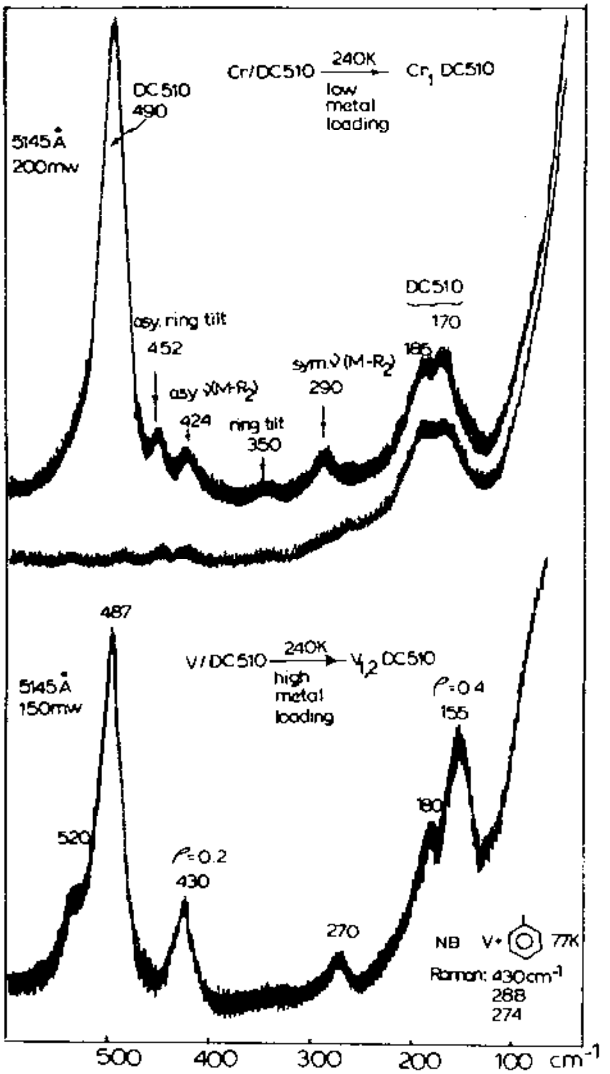

Fig. 10. Raman spectra of Cr/DC510, deposited at 240 K, recorded at 100 K, low Cr loading, mononuclear conditions, parallel and perpendicular polarizations (upper two traces); V/DC510, deposited at 240 K, recorded at 100 K, high V loading, binuclear conditions (ref. 28).

benzene ring rotational motions are frozen out. In relation to polymer supported bis(arene) vanadium, the lower symmetry of the arene rings together with constrained arene rotation, induces anisotropy in the proton coupling which is manifest as line broadening and loss of resolution of the proton superhyperfine lines (Fig. 11A). Computer simulation of the polymer ESR spectra in the rigid support limit has been carried out and their static effective spin Hamiltonian tensor components found to be $g_{\parallel} = 2.025$, $g_{\perp} = 2.030$, $A_{\parallel} = 77.5$ G, $A_{\perp} = 87.8$ G [28,38]. The values for $A_{\parallel}$ and $A_{\perp}$ for polymer supported bis(arene) vanadium are in agreement with the literature values for unsupported bis(arene) vanadium complexes, $\langle A \rangle = 1/3(A_{\parallel} + 2A_{\perp})$ and $\langle g \rangle = 1/3(g_{\parallel} + 2g_{\perp})$ [31]. It is noteworthy that ESR signals from polymer samples containing both the bis(arene) vanadium and divanadium are essentially the same as those described above, implying diamagnetism and ESR silence for the V–V bonded dimer species.

A series of recent experiments that have allowed us to evaluate the role of the support in the growth and stabilization of low nuclearity clusters in

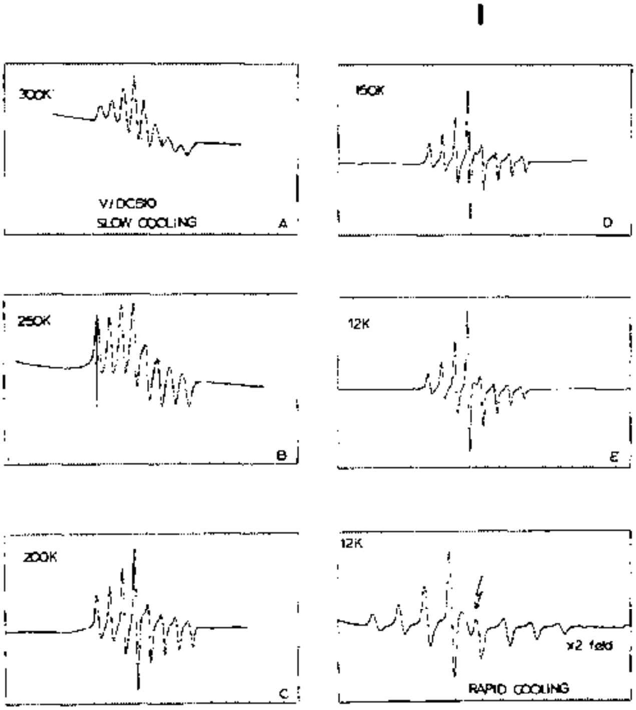

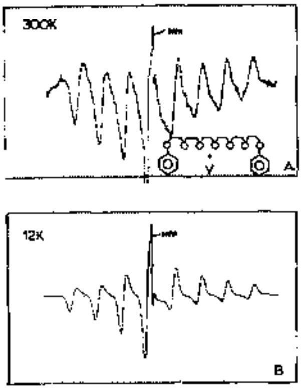

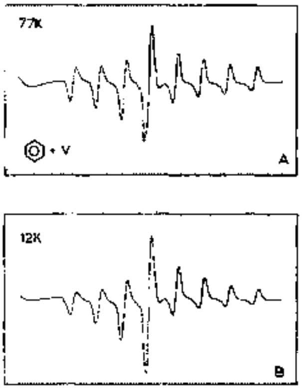

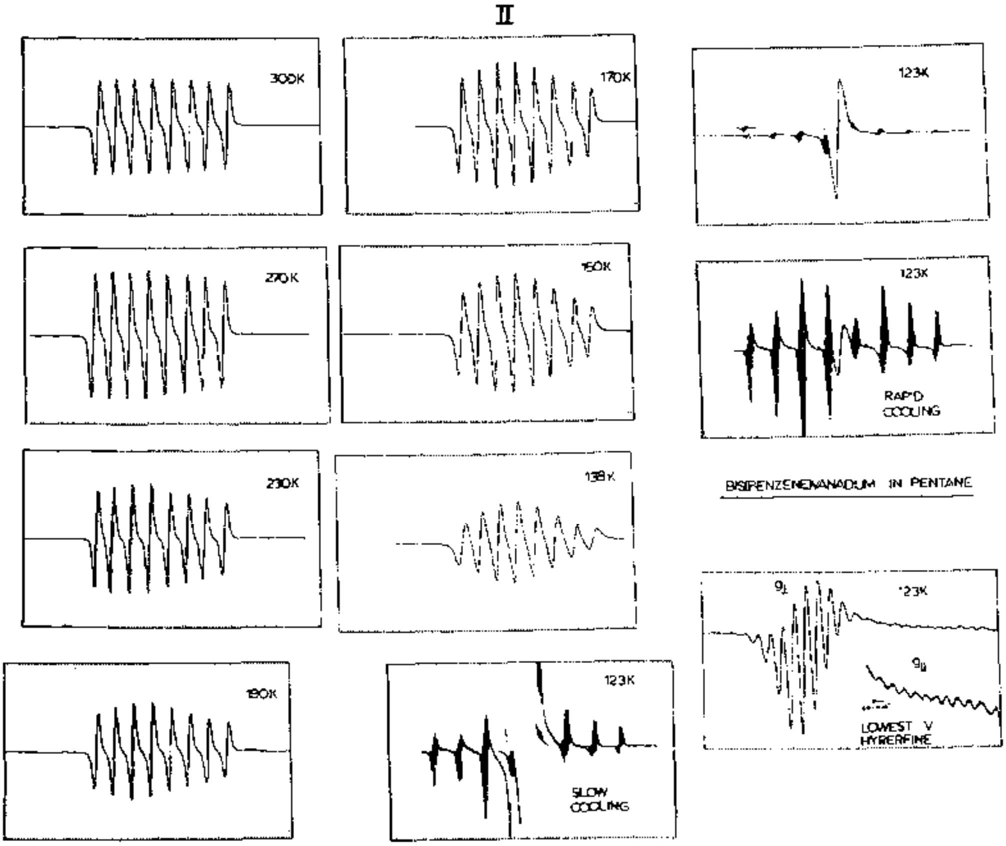

Fig. 11. (I) Temperature dependent ESR spectra of V/DC510, under mononuclear conditions, from 300–12 K, slow and rapid cooling; V/α,ω-diphenylhexaethyleneoxide, 300 and 12 K; V/C_6H_6 prepared at 77 K and recorded at 77 and 12 K. (II) Temperature dependent ESR spectra of bis(benzene) vanadium in pentane at 10^{-4} molar, from 300–123 K (refs. 28,38).

DC510 [32] is summarized in Fig. 12. From these experiments one learns that phenyl substituents, a solvating medium and a bis(arene) metal centre are all necessary for the production and immobilization of arene metal clusters with nuclearities greater than two. This has allowed us to formulate a model that explains the growth of $n = 2, 3, 4, 5$ clusters in the Mo/DC510 polymer. In this agglomeration scheme, a diffusing Mo atom is seen as adding across a Mo$\equiv$Mo quadruple bond of the dimer to give the $n = 3$ clusters, which formally still has a Mo$\equiv$Mo triple bond and which is stabilized by both arene and ether coordination (Fig. 12). In the α,ω-diphenylhexaethyleneoxide having a seven ether oxygen backbone, this system if intramolecular, can go no further than $n = 3$ (Fig. 12), as is found experi-

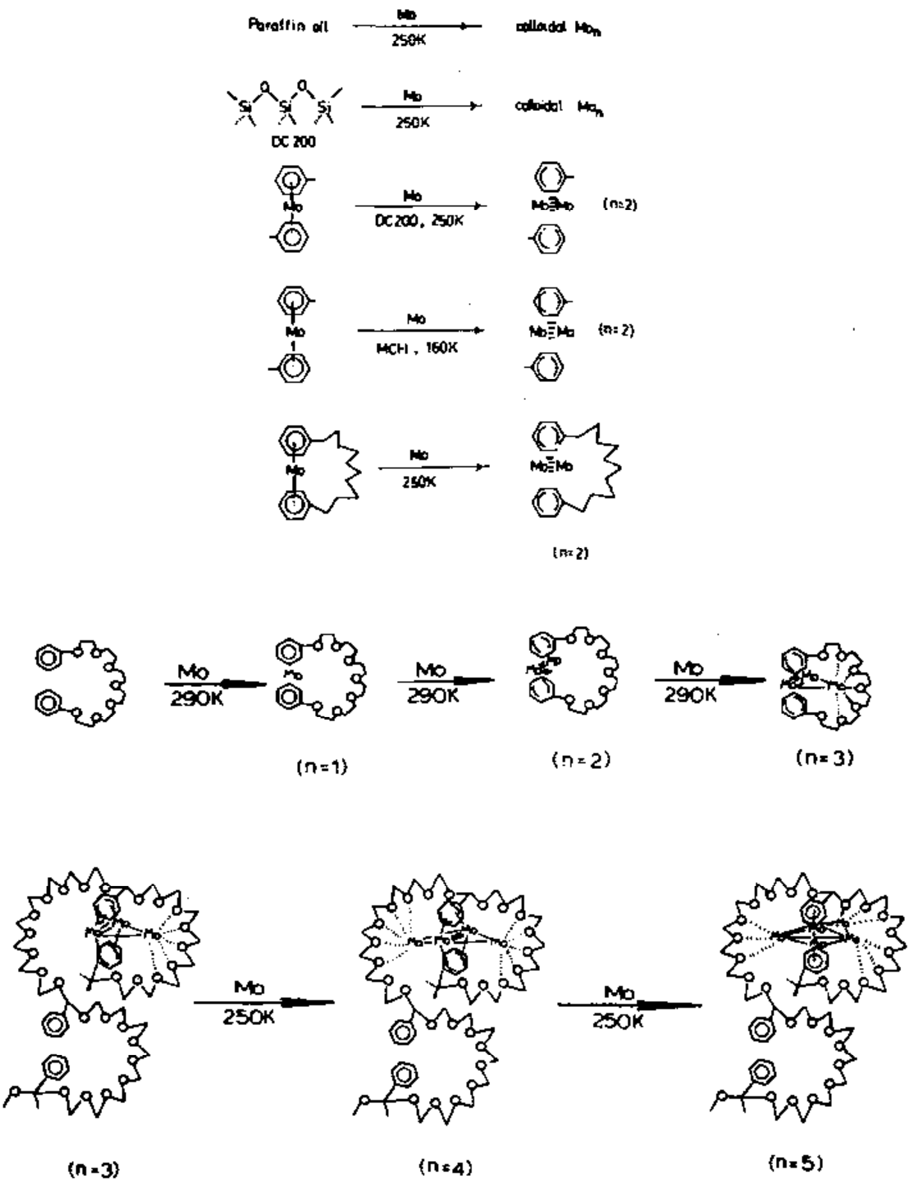

Fig. 12. Matrix and macroscale metal vapor synthetic strategy used to elucidate the role of arene groups, bis(arene) metal centres and oxygen solvation in the Mo/DC510 reaction (ref. 32).

mentally (Fig. 5). On the other hand, in the poly(dimethyl-co-phenylmethyl)siloxane with its larger number of arene functionalities, solvating sites and solvating cavities (Fig. 12) a diffusing Mo atom can further add across the proposed Mo≡Mo triple bond of the trimer to give the $n = 4$ cluster and then across the remaining Mo=Mo double bond of the tetramer to give the $n = 5$ cluster (Fig. 12). This description accounts rather nicely for the observed maximum nuclearity of $n = 5$ attainable in the Mo/DC510 system and the agglomeration order [15]. It also provides a logical explanation for why the bimolecular thermal agglomeration reaction of the $(\text{arene})_2\text{Mo}_2$ species on the polymer produces an unstable (unsolvated) form of the tetramer, compared to the stable (solvated) form produced in the cluster growth process.

These kinds of experiments have recently led, on a microsolution scale, to a successful method of separating the dimer from the monomer [32]. We found that only $(\text{arene})_2\text{Mo}_2$ is produced when $(\text{arene})_2\text{Mo}$ is dissolved in phenyl free liquid poly(dimethyl)siloxane, DC200 (the physical characteristics of which closely match those of DC510) and reacted with Mo atoms. Because of the low vapour pressure of DC200 at 290 K, separation of $(\text{arene})_2\text{Mo}$ from $(\text{arene})_2\text{Mo}_2$ can be achieved by simply pumping the more volatile $(\text{arene})_2\text{Mo}$ complex out of the DC200, leaving the $(\text{arene})_2\text{Mo}_2$ behind.

C. (i) KINETIC MODEL FOR METAL CLUSTER GROWTH IN DC510

In one simple approach [38] one considers the initial step to involve a chain propagation and/or cross linking process in which single metal atoms are captured in a concerted event by phenyl-pairs to produce a polymer supported bis(arene) complex, as illustrated in Fig. 13. These mononuclear sites proceed to act as metal nucleation centres for subsequent metal cluster growth steps

$$\text{L} \ldots \text{L} \xrightarrow[k_{\text{M}}]{\text{M}} \text{ML}_2 \xrightarrow[k_{\text{M}}]{\text{M}} \text{M}_2\text{L}_2 \xrightarrow[k_{\text{M}}]{\text{M}} \ldots \text{M}_j\text{L}_2$$

In this model we have assumed:

(a) L_2 capture sites;
(b) constant concentration of M_jL_2 sites ($j = 0$ to n);
(c) mobile M with diffusion controlled encounters described by rate constant k_{M};
(d) no dissociation of M_jL_2 species, $j \geqq 1$;
(e) constant source of M (R atoms $\text{cm}^2\ \text{s}^{-1}$);
(f) $[\text{L}_2]_{j=0} \gg [\text{M}_j\text{L}_2]$;
(g) low, approximately constant steady-state concentration of free [M];
(h) constant fraction of $[\text{M}_0]$ passing to M_jL_2 species (constant colloid sink term, if required).

With these conditions (judged reasonable from the accumulated background experimental observations) the clustering process can be represented

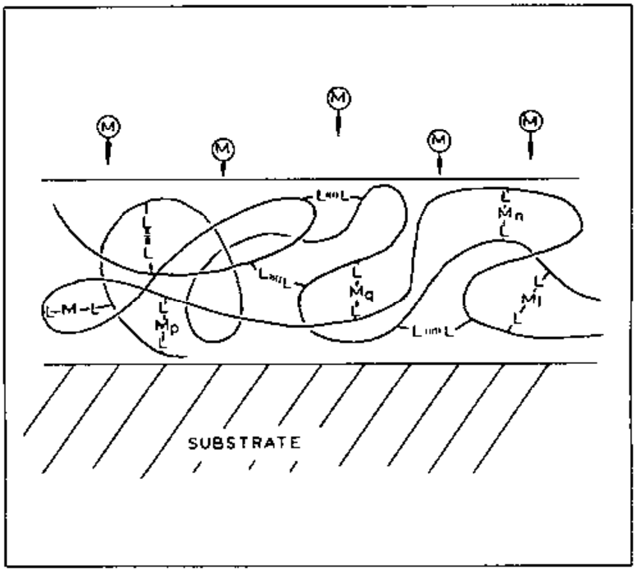

Fig. 13. Model used to analyse the kinetics of metal cluster growth in DC510 (ref. 38).

by the set of differential equations shown below

$$\frac{\mathrm{d}[\mathrm{M}]}{\mathrm{d}t} = R - \sum_{j=0}^{n} k_{\mathrm{M}}[\mathrm{M}][\mathrm{M}_j\mathrm{L}_2]$$

$$\frac{\mathrm{d}[\mathrm{M}_j\mathrm{L}_2]}{\mathrm{d}t} = k_{\mathrm{M}}[\mathrm{M}]\{[\mathrm{M}_{j-1}\mathrm{L}_2] - [\mathrm{M}_j\mathrm{L}_2]\}$$

In solving the differential rate equations, cluster development is envisaged to evolve continuously throughout the time τ in the film (defined as the metal atom deposition period) before the metal atom reacts, after which time the cluster growth, by means of the accretion of metal atoms, is assumed to be quenched and amenable to a time independent spectroscopic observation. The metal atom deposition is then continued for a selected period of time after which the product distribution is recorded again. Product concentration $[\mathrm{M}_j\mathrm{L}_2]$ versus reaction time (metal concentration) profiles can therefore be plotted. A typical example of such a titration is shown in Fig. 14A for V/DC510. In this way every increment of metal deposited into the polymer liquid film in time τ, represents an individual and useable metal concentration measurement $R\tau/\mathrm{vol}^{-1}$. The general solution for the concentration of a cluster species $[\mathrm{M}_n\mathrm{L}_2]$ to the reference mononuclear species $[\mathrm{ML}_2]$ on the polymer is given by:

$$\frac{[\mathrm{M}_n\mathrm{L}_2]}{[\mathrm{ML}_2]} = [\mathrm{M}_0]^{n-1}\frac{2^{n-1}}{n![\mathrm{L}_0]^{n-1}} = K[\mathrm{M}_0]^{n-1}$$

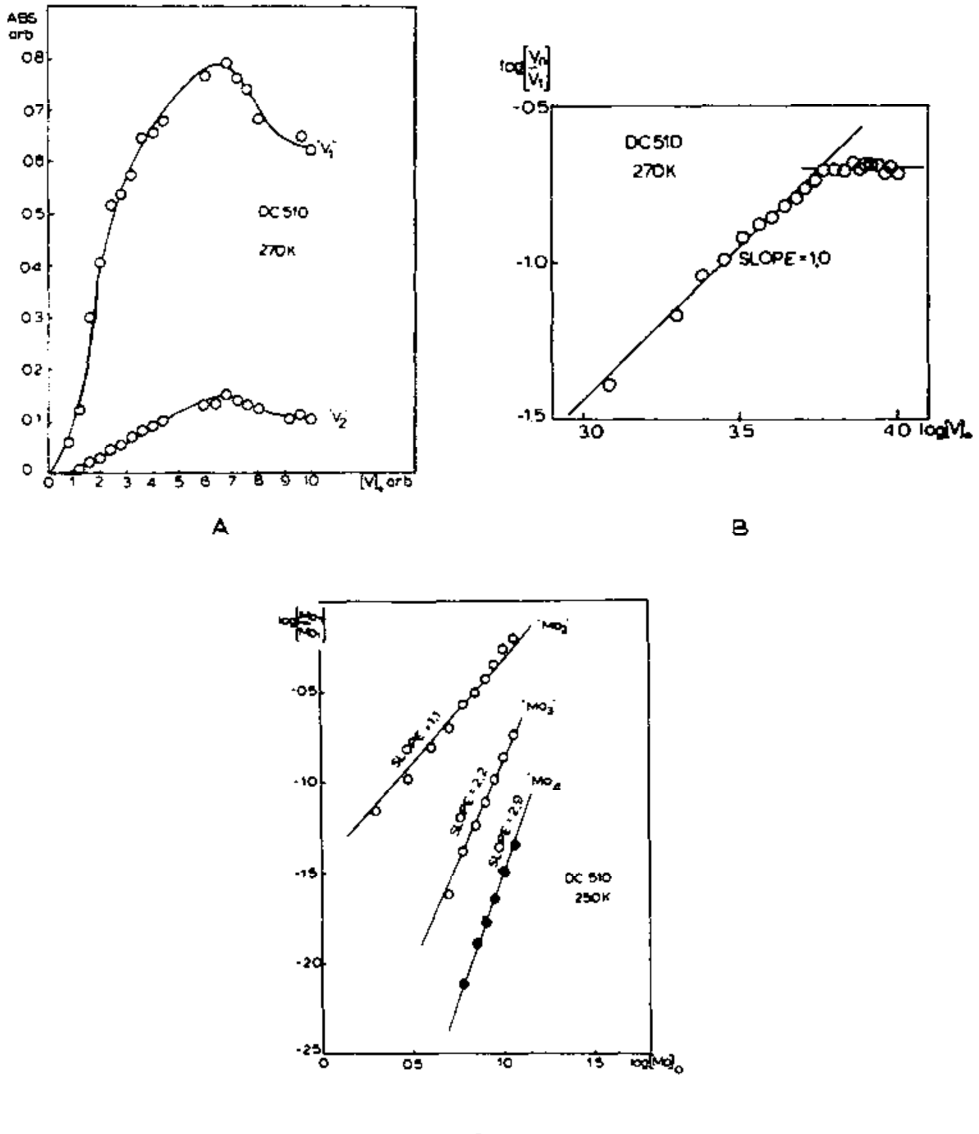

C

Fig. 14. (A) Product concentration $[M_jL_2]$ versus time (or metal concentration) in the V/DC510 reaction at 270 K. (B), (C) $\text{Log}[M_jL_2]/[ML_2]$ versus $[M_0]$ plots for V/DC510 and Mo/DC510 at 250 K (see text for details of the kinetic analysis for determining cluster nuclearity (ref. 32)).

where K is a constant term and $[M_0]$ is the total mass of metal atoms deposited into the polymer film in time τ, which can be used to establish the nuclearity of an unknown cluster product.

This simple analysis predicts that in a less than 1% metal loading limit, after deposition time τ, the absorbance ratio of an unknown nuclearity cluster species M_nL_2 relative to that of the bis(arene) metal complex ML_2 (the latter serving as a mononuclear reference product) should be proportional to the amount of metal $[M_0]$ deposited into the polymer film, raised to the power $(n-1)$. The slopes of $\log[M_nL_2]/[ML_2]$ versus $\log[M_0]$ plots should yield values of $(n-1)$ and hence a spectroscopic probe into cluster nuclearity n. A series of experiments performed on the V_n/DC510, Cr_n/DC510 and Mo_n/DC510 systems [32] appears to conform reasonably well to this simple kinetic model (see for example, Fig. 14B,C) for V, $n=2$; Cr, $n=2$, 3 and Mo, $n=2$, 3, 4 and can be considered to provide a useful method for inferring metal cluster nuclearities from observed spectroscopic features.

C. (ii) THERMAL AGGLOMERATION KINETICS FOR Mo_n/DC510

Viscometry, and thermal agglomeration studies pertaining to the Mo/DC510 system, eludicate among other factors, the role played by inter- and intramolecular crosslinking via bis(arene) molybdenum complex formation, in stabilizing higher nuclearity metal clusters in the order $n=2>3>4>5$ [15,32]. Loss of the binuclear $(arene)_2Mo_2$ species supported on DC510, through diffusion controlled aggregation has been found to follow well behaved second order kinetics [32] (Fig. 15A), the rate for the process and activation energy (Fig. 15B), being functions of metal loading (variations in arene cross link density and oxygen solvation). Thus the activation energy for the dimerization of DC510 supported $(arene)_2Mo_2$ in a low metal loading limit (note that bis(arene) molybdenum is unreactive under these conditions) is 4.2 kcal mol^{-1} compared with a high loading limit value of 14.2 kcal mol^{-1}. The respective diffusion coefficients (290 K) of 32.6×10^{-16} and 18.7×10^{-16} $cm^2\ s^{-1}$ reflect the microscopic mobility of the polymer support, constrained by crosslinking and solvation, to mediate aggregation. These data, together with ESR, EXAFS, SIMS and Raman spectroscopy collectively indicate that the metal cluster growth/agglomeration characteristics in the polymer are determined by a number of effects including:

(i) the presence or absence of covalently bound arene groups;

(ii) changes in the microenvironment in the vicinity of the metal aggregate; cluster size and stability are seen as determined in part by the dimensions and arene density of solvating cavities;

(iii) diffusional encounters are controlled by the polymer microdynamics which are both temperature and crosslink density dependent;

(iv) diffusional limitations will effect the rate at which metal atoms penetrate into the polymer to contribute to cluster growth;

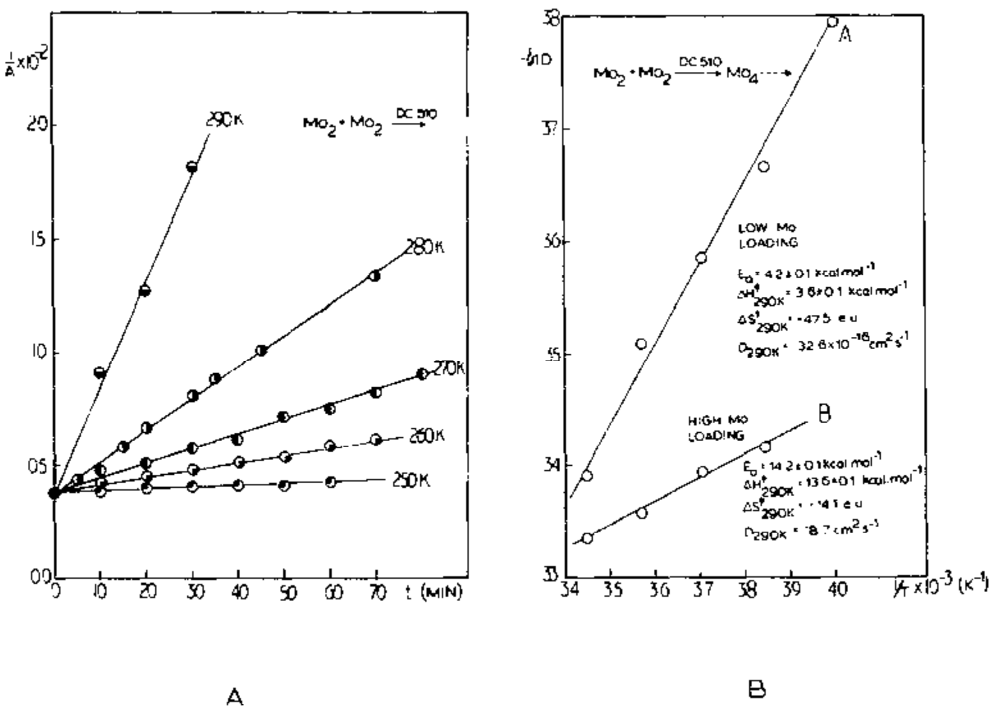

Fig. 15. (A) Bimolecular kinetics of the (arene)$_2$Mo$_2$ dimerization reaction in DC510 at 250, 260, 270, 280 and 290 K. (B) Arrhenius behaviour of the (arene)$_2$Mo$_2$ dimerization for both low and high Mo loading Mo/DC510 (ref. 32).

(v) structural changes or constraints imposed on the metal aggregates or the polymer as a result of binding or stabilization of macromolecules by crosslinking; such changes will control both the number and size distribution of clusters, determining a maximum metal loading limit beyond which metal colloid formation becomes the favoured process for metal atom consumption.

An idealized physical-chemical picture emerges from the results collected to date as shown in Fig. 16. Here, the bis(arene) metal complexes are viewed as cross-linking and/or chain propagating agents, as well as metal nucleation sites for the production of clusters through an array of parallel, competitive metal atom addition reactions. The stable aggregates in the case of V, Cr and Mo appear to require two arene rings and are unsolvated for $n = 2$ (Fig. 16, III) and solvated for $n = 3$, 4 or 5 (Fig. 16, I), by oxygens of the oligomer or polymer backbone. Evidence suggests this interpretation is more likely than the alternate one involving crown ether or cryptand like interactions (Fig. 16, II) without participation of the phenyl substituents.

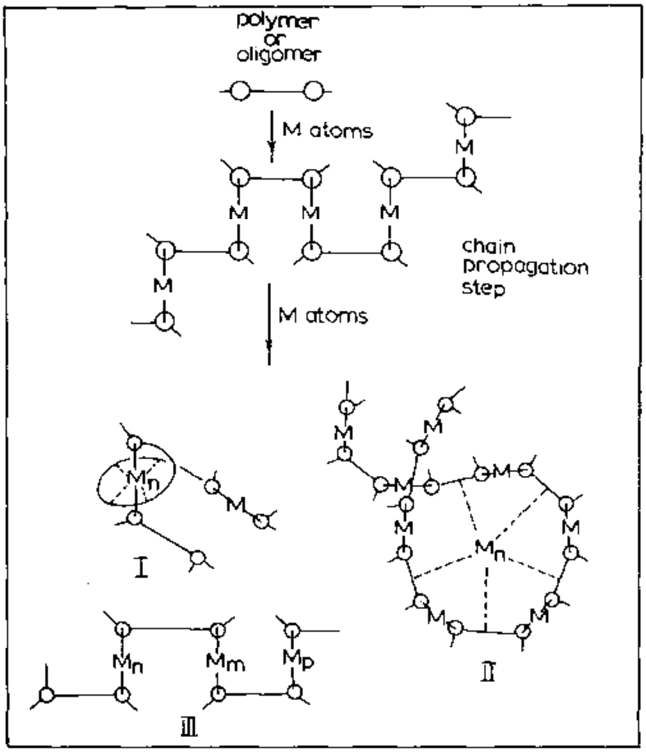

Fig. 16. Illustration of proposed metal atom induced chain propagation and/or cross-linking process for M/oligomer, M/polymer reactions with possible schemes (I, II, III) for the growth and stabilization of metal clusters (refs. 23,32).

D. REACTIONS OF METAL ATOMS WITH CYCLOPENTADIENE FUNCTIONALIZED SILANES, OLIGOMERIC AND POLYMERIC SILOXANES

The rather novel chemical discoveries found for the phenyl functionalized oligomeric and polymeric ethers and siloxanes encouraged us to investigate other ligands. In this section we will briefly describe our progress to date with cyclopentadiene (Cp) functionalized silanes and siloxanes. This choice of substituent was based in part on literature successes with Cp metal derived catalyst systems of both a homogeneous and hybrid type [33]. However, the literature on Cp hybrid phase catalysts is presently quite sparse. The few solid phase systems that have been reported, show promise for a variety of catalytic transformations (Fischer–Tropsch, N_2 reduction, olefin oligomerization etc.). Difficulties with these solid phase catalysts concern the characterization of active metal centres, and the incorporation of sufficient ligand mobility to allow specific Cp metal complexes to form but at the same time minimizing agglomeration of Cp metal sites and Diels–Alder cross-linking of Cp groups. Pez's [34] recent stabilization of the reactive titanocene monomer by coordination to diglyme, exemplifies some of the benefits of solvating sites. Liquid Cp polysiloxanes were therefore considered as interesting ligands for MVS, possibly providing a route to liquid phase Cp-functionalized catalyst systems, in which the active sites could be amenable to specific tailoring and precise characterization.

Our metal vapor-liquid and solution phase Cp silane and siloxane chemistry to date is proving to be rich in novel reactions and unexpected results [35].

The first point of chemical interest to emerge from the Cp project concerns the reaction of some first row metal atoms with cyclopentadiene itself (Fig. 17). Comparing solution phase and cocondensation experiments, it is evident that in the case of cobalt, the cocondensation technique yields the "less oxidized" product, whereas in the solution phase, the reaction proceeds to the "more oxidized" product, cobaltocene. The oxidizing mechanism is thought to be hydride abstraction by either incoming cobalt atoms,

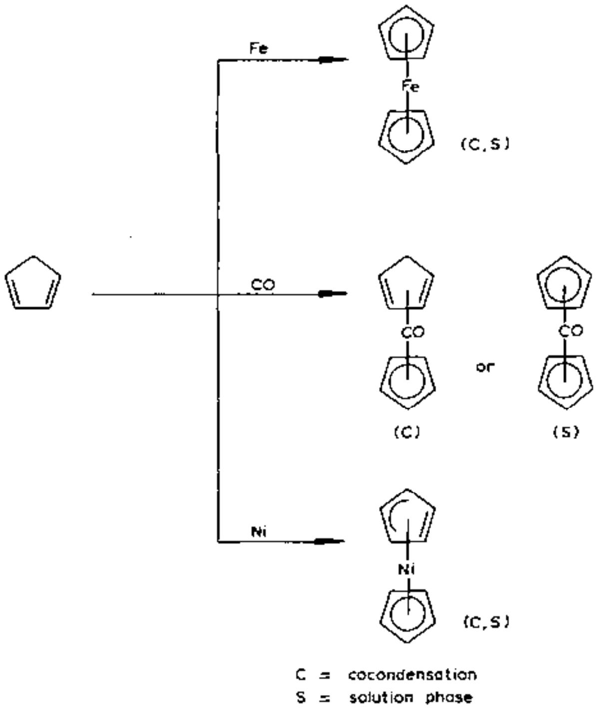

Fig. 17. Metal vapor cocondensation and solution phase reactions with cyclopentadiene (ref. 35).

or by an intermolecular process in solution [36]. Unfortunately, no evidence for metal hydride intermediates or η^4–η^4 Cp-diene intermediates was observed in these systems, although bis-diene metal complexes have been found to form readily in the reactions of 1,5-cyclooctadiene (1,5-COD) with Fe, Co and Ni in methylcyclohexane solution at − 120°C. The $(1,5\text{-COD})_2M$ complexes are stable to about − 50°C in the case of Fe and Co, and stable at room temperature in the case of Ni [14]. As a model for the reactivity patterns of Cp–Si groups in oligomeric and polymeric siloxanes the metal vapour chemistry of trimethylsilylcyclopentadiene, $C_5H_5SiMe_3$, was investigated with Fe. The Me_3SiCp ligand is known to be a fluxional molecule undergoing H atom migrations around the Cp ring to produce an equilibrium distribution of 90 : 9 : 1 for the 5, 1 and 2 isomers respectively (^1H, ^{13}C and ^{29}Si NMR). Thus under the conditions of our experiment the 5-isomer is expected to predominate. Interestingly the reaction of Fe atoms with Me_3SiCp/MCH at 150 K yielded a dark green product rather than an orange one for the anticipated $(\eta^5\text{-}C_5H_4SiMe_3)_2Fe$ ferrocene derivative. However, warming to room temperature under oxygen yielded the ferrocene product as shown in Fig. 18A. Proof of the nature of the green precursor product derived from the similarity of its microsolution optical spectrum (as well as the corresponding bis(trimethylsilyl)cyclopentadiene derivative) to that of the 16 electron $(1,5\text{-COD})_2Fe$ (Fig. 18B) and its chemical reactions with CO and PMe_3 to yield the bis-diene carbonyl complex and the mono-diene tris-phosphine complex respectively, as illustrated in Fig. 18A. These results collectively point towards the green product as being a 16-electron bis-diene iron (0) complex. The enhanced stability of η^4-Cp complexes in the order:

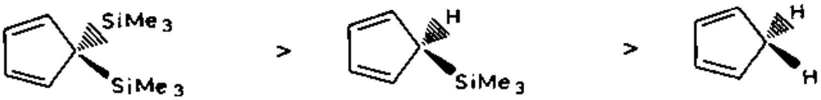

is speculated to be either a steric and/or electronic effect of the Me_3Si substituent.

Reactions of Fe atoms with model Cp-siloxane oligomers were considered useful precursor studies to the Cp-siloxane polymers, where again Fe was the metal of choice. With the 1,3-cyclopentadiene–1,1′,2,2′,3,3′-hexamethyltrisiloxane ligand, monomeric, oligomeric and polymeric products involving intra- and intermolecular Cp_2Fe crosslinking groups were anticipated and indeed observed, as summarized in Fig. 19. Products were generally manipulated at low temperatures and characterized by a combination of UV–visible, mass and NMR spectroscopy, as well as a gel permeation chromatographic estimation of their molecular weights. These analyses indicated that an intramolecular ferrocene monomer, an intermolecular ferrocene closed ring dimer and an intermolecular ferrocene open dimer and trimer were the

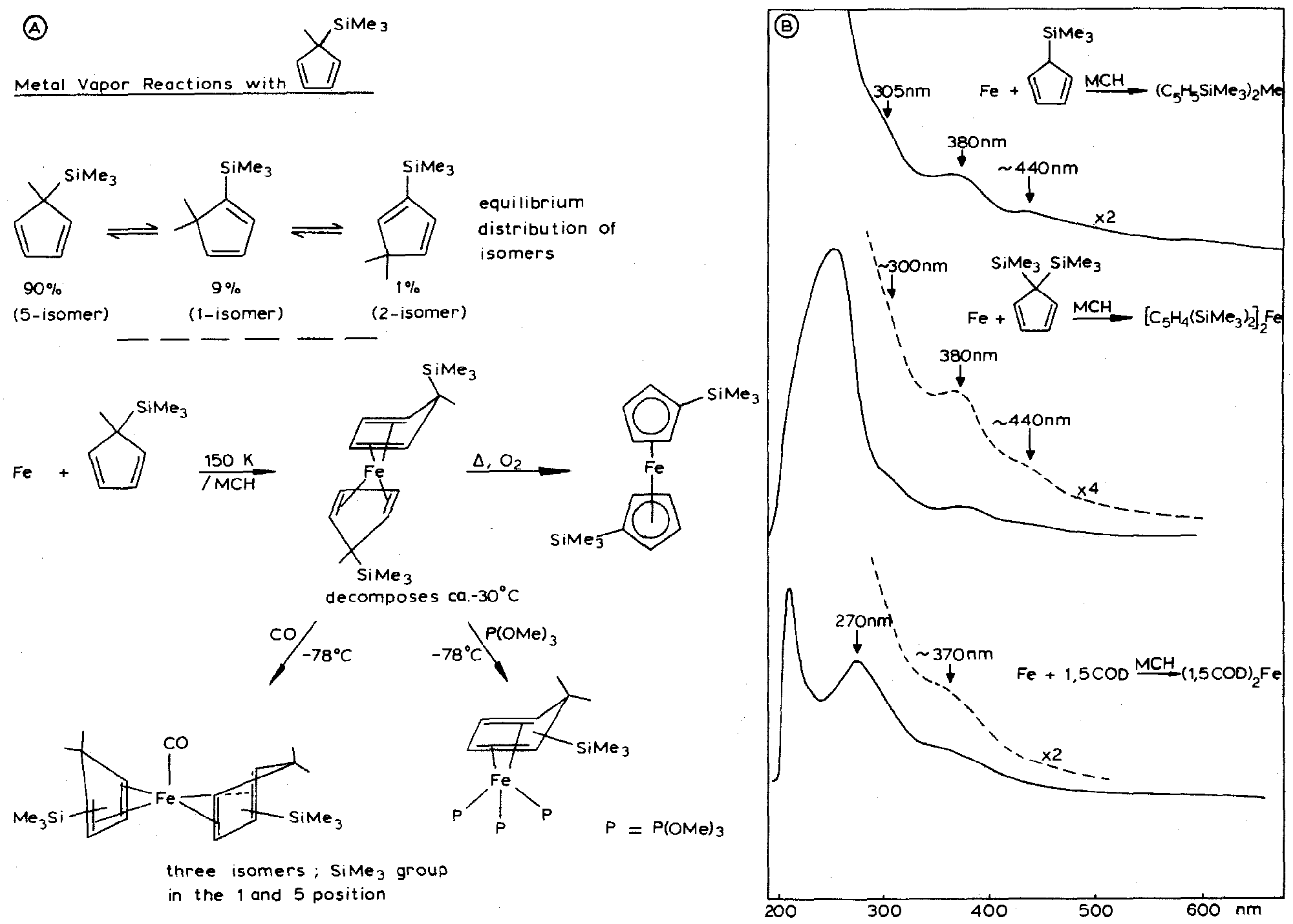

Fig. 18. (A) Iron atom solution phase reactions with $C_5H_5SiMe_3$ in methylcyclohexane (MCH) (10%) at 150 K. (B) UV-visible microsolution optical spectra of the reaction of iron atoms with 10% methyl cyclohexane solutions of $C_5H_5SiMe_3$, $C_5H_4(SiMe_3)_2$ and 1,5 COD at 150 K (ref. 35).

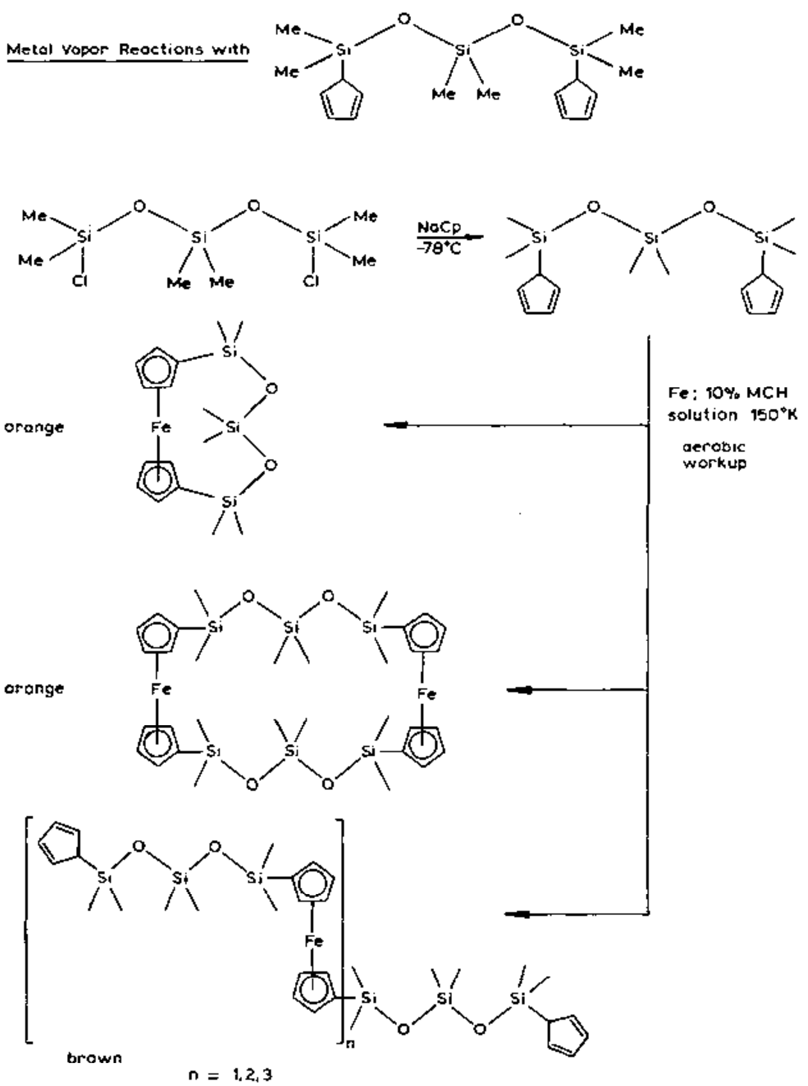

Fig. 19. Iron-atom reactions with 1,3-cyclopentadiene-1,1′,2,2′,3,3′-hexamethyltrisiloxane in methylcyclohexane (10%) at 150 K (ref. 35).

major products (Fig. 19). These model monomer and oligomer studies were important in that they explored the effect of the silicon substituent on the outcome of the metal vapour reaction, and furthermore demonstrated that Diels–Alder reactions leading to Cp dimerization and hence crosslinking of Cp polymers could be kept at a usefully low level, by low temperature manipulation of reagents and products. On the other hand, it should be noted that the Diels–Alder effect could be exploited to produce desirable crosslinked, solid Cp-siloxane polymers containing Cp-metal sites.

The ground work had then been laid for Cp-siloxane polymer synthesis which led us into essentially virgin territory. A number of different approaches to desirable Cp-siloxane polymers have been evaluated in our work. A method which allows fairly ready manipulation of polymer viscosity by varying the MW of the starting polymer and the bulkiness of the alkyl side

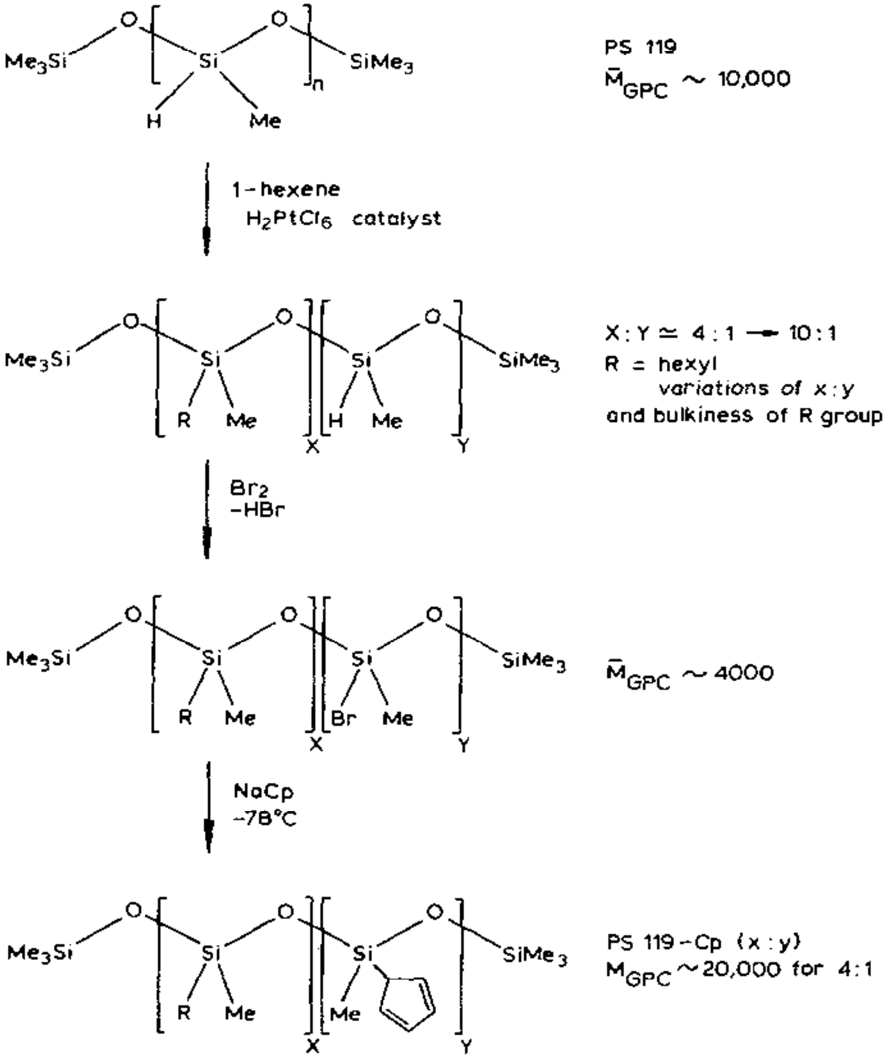

Fig. 20. A scheme for the synthesis of cyclopentadiene functionalized siloxane polymers (starting polymer, PS 119, supplied by Petrarch) (ref. 35).

chain, involves a methylhydrosiloxane liquid polymer precursor and a synthetic strategy as laid out in Fig. 20. The MW of the polymer and its NMR characterization were necessary to judge the progress of each step in the synthesis. A useful aspect of this synthesis, is that the crucial choice of Cp loading on the polymer ($x:y$) is determined by the initial choice of hydrosilation conditions.

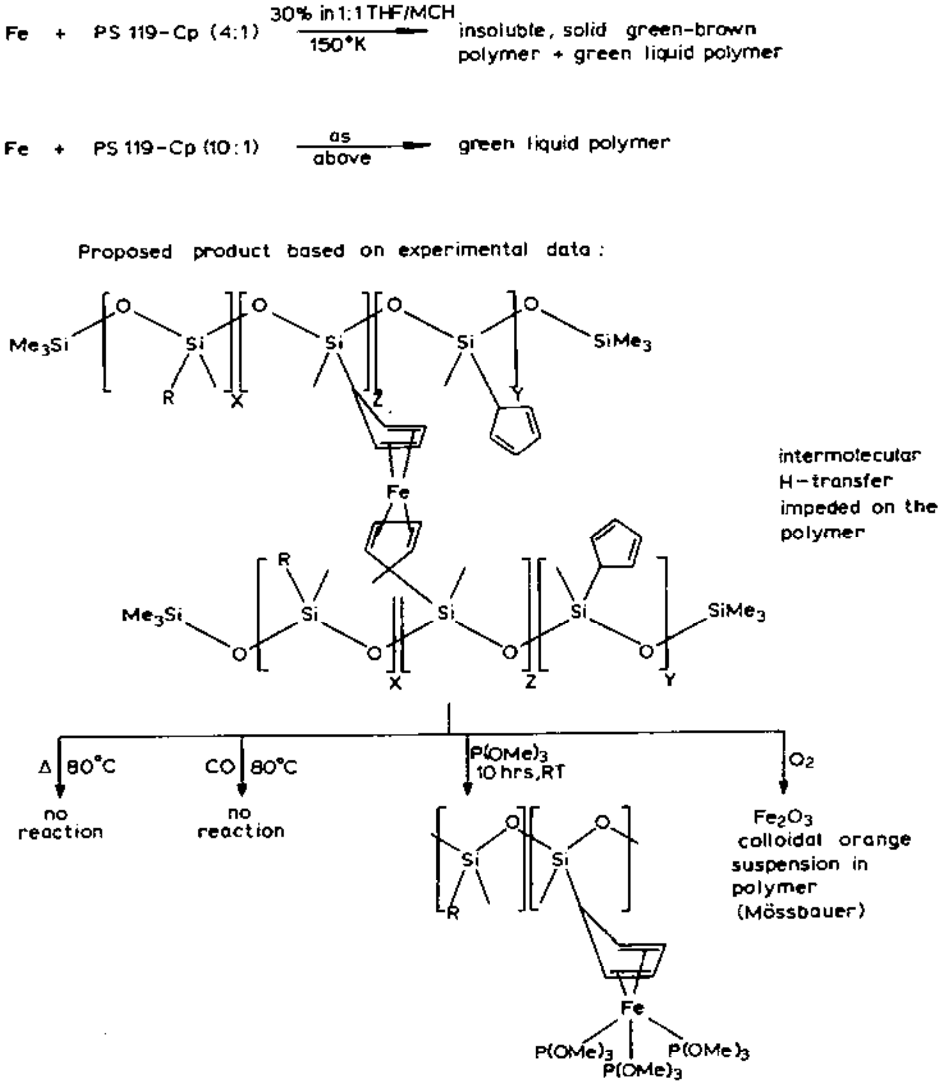

Fig. 21. Iron atom-solution phase reactions with cyclopentadiene functionalized siloxane polymers (ref. 35).

The reactions of Fe atoms with Cp-siloxane polymers were performed with a solution of the polymer in THF/MCH (1 : 1) at 150 K to avoid thermal crosslinking induced by radiation heating from the metal evaporation source. In all cases studied so far, the products were either green liquid polymers or insoluble solid green polymers. The optical and Mössbauer spectroscopy of the products as well as their thermal and oxidative behaviour and reactions with CO and PMe_3, summarized in Fig. 21, lead us to believe that the iron site on the polymer is in the form of a sixteen electron, bis-diene iron (0) complex. The enhanced thermal stability of the polymer anchored iron diene complex compared to that of the $(\eta^4\text{-}C_5H_5SiMe_3)_2Fe$ monomer can be accounted for by postulating an intermolecular hydrogen transfer mechanism in the transformation of the diene to the ferrocene derivative. Thus, the rigid nature of the Cp-polymeric ligand would inhibit this process and hence prevent conversion to the ferrocene derivative. Instead the system tends to oxidize to Fe_2O_3 in oxygen rather than to the ferrocene product. Complete details of this work will be published soon.

Collectively, the results obtained so far with Fe atom Cp-siloxane polymer reactions, as well as with other metal atoms, indicate that the approach can be used to synthesize and stabilize polymer supported cyclopentadiene and cyclopentadienyl metal complexes. Critical parameters in the choice of polymer precursor certainly involve MW, viscosity, Cp-density and steric bulk of alkyl substituents.

E. REACTIONS OF SILVER ATOMS WITH OLIGO AND POLYOLEFINS; POLYMER PROTECTED METAL COLLOIDS

Conventionally the production and stabilization of charged and zero-valent silver particles is accomplished by reduction (γ-radiolysis, hydrogen, dye sensitization, photolysis) of silver cations in media that range at one extreme from fluid room temperature solvents, to rigid glasses and crystals at the other [4,37]. Silver particles ranging in size from a single silver atom, to low nuclearity Ag_n ($n = 2$–20) clusters, to species of colloidal dimensions are detectable in particle populations which can show considerable variation in time, both in dispersion and stability towards agglomeration. Very recently, we have devised an alternate direct route to colloidal and subcolloidal silver which utilizes the technique of silver atom-liquid phase chemistry [38]. Principally we have found that when atomic silver is deposited at carefully controlled rates in vacuo into cooled, weakly interacting liquid supports (e.g. polyolefin, oligo-olefin, vinyl and phenyl siloxane polymers, crown ethers and low molecular weight ether solvents) silver particles ($10 < R < 200$ Å) develop with a size dispersion that remains independent of silver loading at a fixed temperature. Apparently, the rate at which Ag is deposited and diffuses in these media, is commensurate with the relaxation time required for solvent, oligomer or polymer conformational reorientation of a protective barrier about a growing particle, in such a way that the particle is prevented from further growth, once it reaches a critical dimension. This effect has been found from our recent studies to manifest itself optically in the linear growth of the relevant plasmon absorption with increasing concentration and in the invariance of the λ_{max} and half-bandwidth ($\Delta\nu\frac{1}{2}$). Particles generated in oligomeric and polymeric olefinic supports show greater stability towards thermally induced agglomeration than do the easily desolvated species produced in low molecular weight liquid solvent media. In general the silver atom experiment, in a matrix cocondensation sense (12–77 K) or a microsolution sense (140–300 K), surveys a wide range of states of silver aggregation, thereby providing opportunities to study the evolution of colloidal silver from silver atoms and clusters. These stages of evolution can in principle be examined in sufficient detail to permit, for example, analysis of the onset of the controversial quantum size effects in the optical and ESR properties of small silver particles, [39] and an experimental assessment of the range of validity of the classical Mie theory in the small particle scattering limit [40]. In addition, such studies are also stimulated by interest in assessing the role such dispersions may play as photoredox systems for energy deposition, charge separation and H_2 generation. Following some of our earlier 12 K Ag_n/olefin matrix studies involving ethylene, propylene and but-1-ene [12,41], we have discovered that neat poly(isoprene) films at 255 K (well above the glass transition) are unable to limit colloidal silver to a narrow size regime, as seen by the continuous red-shifting of the plasmon band (420 to 540 nm) and band broadening ($\Delta\nu\frac{1}{2}$, 50 to 264 nm), when the films are exposed to silver atoms at very slow deposition rates Fig. 22A. By contrast, squalene, a low molecular weight liquid analogue of this polymer, when reacted with silver atoms at 260 K, shows an absorption due to Ag_n at 420 nm whose intensity increases linearly with silver loading and whose band width ($\Delta\nu\frac{1}{2}$, 100 nm) and λ_{max} remain invariant (Fig. 22B). The implication is that this oligo-olefin allows Ag and Ag_n to diffuse and agglomerate to a particular size (perhaps 200 Å) and then is removed from further reaction, possibly by adsorption of the organic phase on the particle surface as illustrated in Fig. 22C. Similar behaviour is observed for liquid poly(butadiene) ($\overline{MW} = 900$) silver composites prepared at 294 K (λ_{max}, 415 nm; $\Delta\nu\frac{1}{2}$, 70 nm). The effect of zeolite additives on the growth and stabilization of silver clusters in these liquid polyolefinic supports is currently under investigation. Here it seems that the organic phase could mediate the diffusive transfer of silver atoms and/or clusters into the zeolite, which has interesting implications in the fabrication of silver-zeolites. Furthermore, we have also found that low molecular weight ether and crown

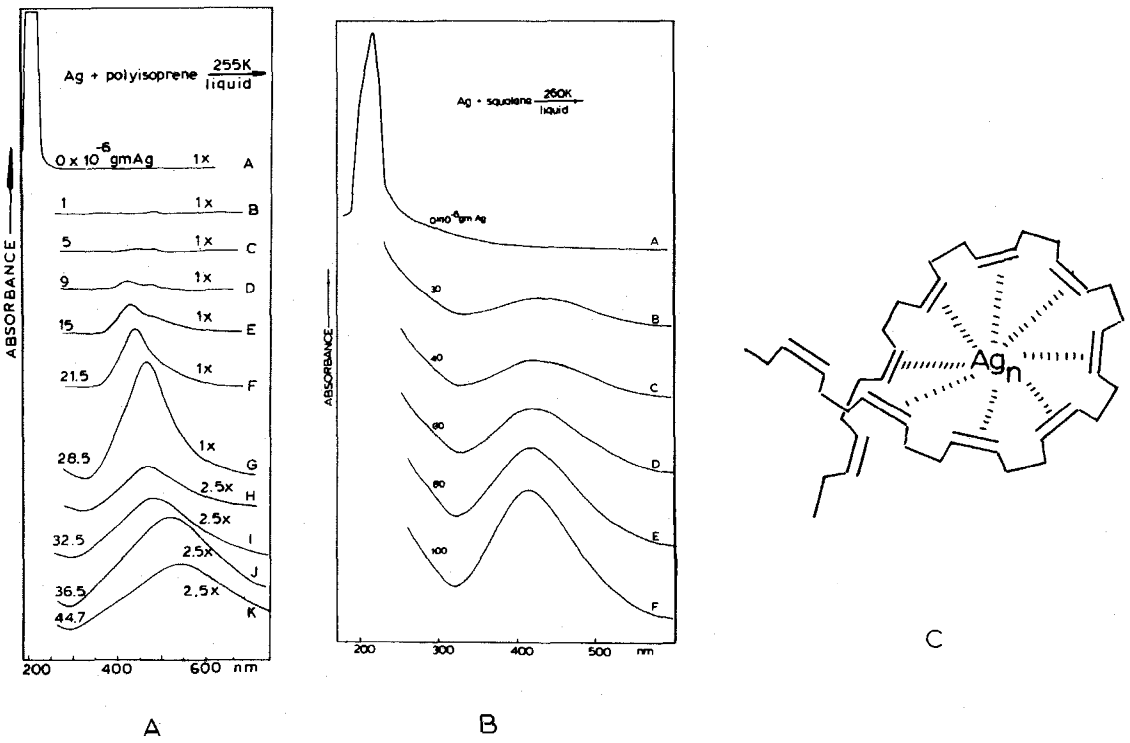

Fig. 22. (A) Silver atom-liquid polyisoprene titration monitored by in situ optical transmission spectroscopy, performed and recorded at 255 K. (B) Similar to (A) but for liquid squalene at 260 K. (C) Pictorial representation of a polyolefin solvating void for stabilizing silver cluster monodispersions in a liquid oligo- or polyolefin (ref. 38).

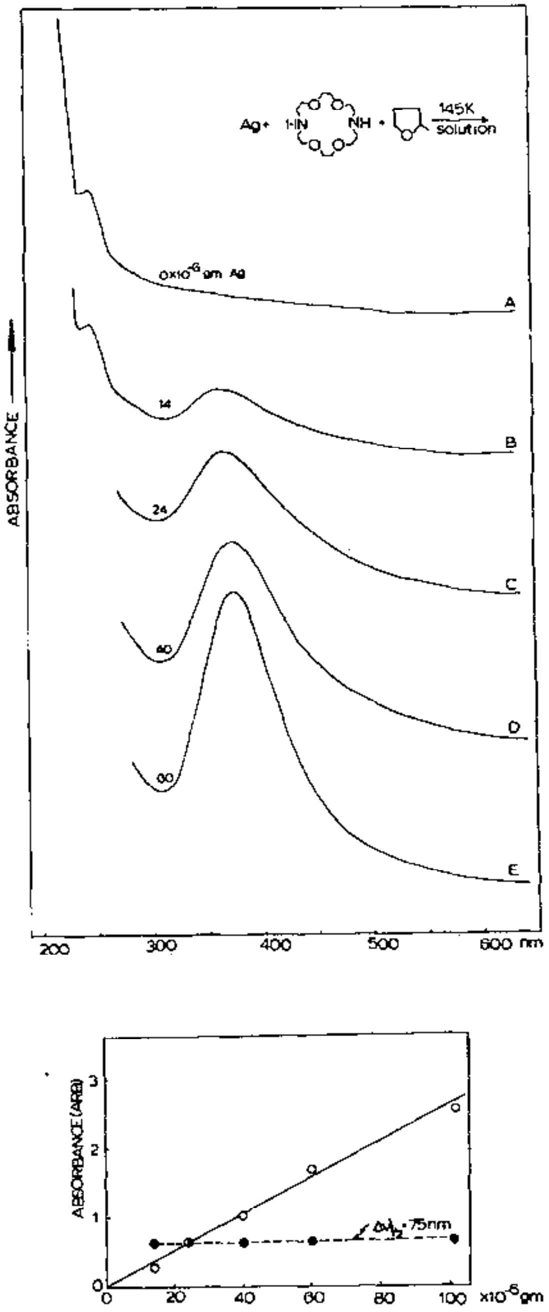

Fig. 23. Similar to Fig. 22 but for liquid 2-methyl-tetrahydrofuran /5% 1,10-diaza-18-crown-6 at 145 K; the insert shows a graphical representation of the silver atom concentration dependence of the plasma resonance absorption and respective band width (ref. 38).

ether/solvent systems support the growth of stable Ag_n dispersions. For example in 2Me-THF, proportional growth is again observed (145 K, λ_{max} 410 nm, $\Delta\nu\frac{1}{2}$ 120 nm) but with a broadened particle size distribution than those produced in squalene at 260 K or poly(butadiene) at 294 K. The silver particles, probably stabilized by the solvent against further agglomeration, appear to be able to diffuse together to form larger particles (plasmon red-shifting, band broadening) quite readily when the temperature of the solvent is raised 10–20°C. It is noteworthy, that when 1,10-diaza-18-crown-6 is incorporated in 2Me-THF, the λ_{max} for the optical process shifts to 375 nm with $\Delta\nu_{1/2}$, 75 nm (Fig. 23). Moreover, the optical absorption of this Ag_n species grows in intensity at a rate approximately twice that observed in squalene. These observations indicate that the aza-crown ether does participate in the cluster growth and stabilization process, possibly in a sandwich coordination mode as observed recently for Na^+ cations with bridged aza-crown ethers [21]. However, the thermal stability of the silver aggregates is not enhanced by the presence of the aza-crown ether over that in 2Me-THF alone. From our experiences so far with polymer protected Ag_n generated by silver atom-liquid phase deposition techniques, it would appear that with a careful choice of support, silver atom growth and stabilization can be controlled to the point of being able to isolate ultrafinely divided, narrow size cluster distributions of a type that cannot be obtained by conventional procedures. These systems are being investigated further, to establish the generality of the technique for other solvating liquids and metals. The long term stability of these systems and potential for catalytic and photocatalytic applications is also being pursued.

F. CONCLUSIONS

To bring metal vapour synthesis out of the cold into the room temperature regime, requires a judicious choice of involatile ligands and/or solvents which may be of a monomeric, oligomeric or polymeric type. Of the many systems examined in the course of our work in this new field, the reaction of Mo atoms with liquid α,ω-diphenylhexaethyleneoxide at 290 K to yield arene-molybdenum clusters up to $n = 3$ and Ag atoms with liquid poly(butadiene) at 295 K to produce a monodispersed silver colloid, should be highlighted as they are examples of metal atom reactions that will only operate at room temperature (lower temperatures favour metal film formation on the liquid). One expects that other reactions of this type will be discovered in future work, some of which could be of technical interest and possible commercial significance. Combined with room temperature metal vapour sources, such as hollow cathode sputtering or magnetron sputtering devices, there appears to be no obvious practical obstacles militating against the large volume production of specialized chemicals and catalysts using metal vapour synthetic methods [10].

ACKNOWLEDGEMENTS

We would like to acknowledge the Natural Sciences and Engineering Research Council of Canada for financial assistance from the Operating, Strategic Energy and PRAI programmes at various stages of the research described in this paper. (M.A.) also wishes to acknowledge the Provincial Government for an OGS at the early stages of his graduate research and (L.N.) thanks NSERC for a scholarship for the duration of her graduate work. The expert design and machining abilities of Mr. Karl Molnar and his colleagues are most sincerely appreciated. Many helpful discussions with Dr. Saba Mattar concerning the interpretation of the ESR spectra are gratefully acknowledged.

REFERENCES

1 K.J. Klabunde, Chemistry of Free Atoms and Particles, Academic Press, New York, 1980; J.R. Blackborow and D. Young, Metal Vapor Synthesis in Organometallic Chemistry, Springer-Verlag, New York, 1979; M. Moskovits and G.A. Ozin, Cryochemistry, Wiley-Interscience, New York, 1976; S. Craddock and A.J. Hinchcliffe, Matrix Isolation, Cambridge University Press, London, 1975 (and references cited therein).
2 R.E. MacKenzie and P.L. Timms, J. Chem. Soc. Chem. Commun., (1974) 650.
3 R. Kellerman and J. Texter, J. Chem. Phys., 70 (1979) 1562.
4 R.H. Humphry-Baker, M. Grätzel, P. Tundo and E. Pillizzetti, Angew. Chem., 91 (1979) 669.
5 M.C.R. Symons and C.E. Forbes, Mol. Phys., 27 (1974) 467.
6 F. Vögtle and F. Weber, Angew. Chem. Int. Ed. Engl., 18 (1979) 753, and references cited therein.
7 K.J. Klabunde, H.F. Efner, T.O. Murdock and R. Ropple, J. Am. Chem. Soc., 98 (1976) 1021.
8 J.R. Blackborow, R. Grubbs, A. Miyashita and A. Scrivanti, J. Organomet. Chem., 120 (1976) C49.
9 C.G. Francis and P.L. Timms, J. Chem. Soc. Chem. Commun., (1977) 466; J. Chem. Soc. Dalton Trans., (1980) 1401.
10 Torrovap Industries Inc., Toronto, Ontario, Canada; Planar Instruments, Oxford, England.
11 H.X. Huber, P. McKenzie and G.A. Ozin, J. Am. Chem. Soc., 102 (1980) 1548.
12 G.A. Ozin, Faraday Symp. Chem. Soc., 14 (1980) 7, and references cited therein.
13 C.G. Francis and G.A. Ozin, J. Mol. Struct., 59 (1980) 55.
14 G.A. Ozin, C.G. Francis, H.X. Huber, M. Andrews and L. Nazar, J. Am. Chem. Soc., 103 (1981) 2453.
15 C.G. Francis, G.A. Ozin and H.X. Huber, Inorg. Chem., 19 (1980) 219.
16 C.G. Francis, G.A. Ozin and H.X. Huber, Angew. Chem. Int. Ed. Engl., 19 (1980) 402.
17 C.G. Francis, G.A. Ozin and H.X. Huber, J. Am. Chem. Soc., 101 (1979) 6250.

18 C.G. Francis and G.A. Ozin, J. Macromol. Sci., Chem., A(1), 16 (1981) 167.

19 G.A. Ozin, E.P. Kündig and G.A. Ozin, Nature (London), 254 (1975) 503; M. Moskovits and J.E. Hulse, J. Chem. Soc. Faraday Trans. 2, (1977) 471.

20 T.A. Ford, H. Huber, W. Klotzbucher, M. Moskovits and G.A. Ozin, Inorg. Chem., 15 (1976) 1666.

21 M.J. Calverly and J. Dole, J. Chem. Soc. Chem. Commun., (1981) 684.

22 M. Andrews and G.A. Ozin, Angew. Chem., 94 (1982) 218.

23 T. Aoki, F. Furusaki and Y. Tomhe, Bull. Chem. Soc. Jpn., 42 (1969) 545.

24 F.A. Cotton, Accounts Chem. Res., 11 (1978) 225; M.H. Chisholm and F.A. Cotton, Accounts Chem. Res., 11 (1978) 356, and references cited therein.

25 P. Montano, private communication (1982).

26 P. Montano, M. Andrews and G.A. Ozin, unpublished work (1981).

27 J. Michl, M. Andrews and G.A. Ozin, unpublished work (1981).

28 M. Andrews and G.A. Ozin, Inorg. Synth., in press.

29 E. Maslowsky, Jr., Vibrational Spectra of Organometallic Compounds, Wiley, New York, 1977, and references cited therein.

30 D.F. Shriver and C.V. Cooper III, in R.J.H. Clark and R.E. Hester (Eds.), Advances in Infrared and Raman Spectroscopy, Heyden, London, 1980, Vol. 7, and references cited therein.

31 G.H. Olive and S. Olive, Z. Phys. Chem., 56 (1967) 223.

32 M. Andrews and G.A. Ozin, Angew. Chem., Suppl., (1982) 1255.

33 J.K. Stille and A. Sekiya, J. Am. Chem. Soc., 103 (1981) 5096; W.D. Bonds, Jr., C.H. Brubaker, Jr., E.S. Chandrasckan, C. Gibbons, R.H. Grubbs and L.C. Kroll, J. Am. Chem. Soc., 97 (1975) 2128; P. Perkins and P.C. Vollhardt, J. Am. Chem. Soc., 101 (1979) 3985.

34 G. Pez, private communication (1981).

35 L. Nazar, G.A. Ozin and C.G. Francis, International Organometallic Conference, Toronto, August 1981, paper 4 D07, J. Am. Chem. Soc., submitted.

36 S. Ittel, J. Organomet. Chem., 195 (1980) 331.

37 P.A. Brugger, P. Cuendet and M. Grätzel, J. Am. Chem. Soc., 103 (1981) 2923; A. Henglein, J. Phys. Chem., 83 (1979) 2209; Ber. Bunsenges. Phys. Chem., 84 (1980) 253; A. Henglein and Th. Proske, Ber. Bunsenges. Phys. Chem., 82 (1978) 471; K. Monserrat, M. Grätzel and P. Tundo, J. Am. Chem. Soc., 102 (1980) 5527; A. Henglein and R. Tausch-Treml, J. Colloid and Interface Sci., 80 (1981) 84, and references cited therein.

38 M. Andrews, S. Mattar, H. Huber and G.A. Ozin, unpublished work (1982).

39 G.C. Papavassiliou, Prog. Solid State Chem., 12 (1980) 185; R.F. Marzke, Cat. Rev. Sci. Eng., 19 (1979) 43, and references cited therein.

40 G. Mie, Ann. Phys., 25 (1908) 377.

41 D. McIntosh, G.A. Ozin and H. Huber, J. Organomet. Chem., 121 (1976) 127; D. McIntosh, G.A. Ozin and R.P. Messmer, Inorg. Chem., 19 (1980) 3321.